The referees' comments are reproduced in black hereafter, and our responses are shown in blue. The track-change manuscript is attached below after the responses.

Anonymous Referee #1

The authors describe the protocol that will be used to compute melt rates at the base of ice shelves in ice sheet models driven by output of global climate models in the framework of the Ice Sheet Model Intercomparison Project for CMIP6 (ISMIP6). The global climate models included in CMIP6 have generally a too coarse resolution and do not simulate explicitly the circulation and fluxes in the ice shelves cavities. It is thus important that all the groups participating in ISMIP6 use a similar protocol to derive the melt rates from those global model results so that the origin of the differences in their results can be more easily investigated.
The manuscript is very clear. It describes precisely and justifies well the choices performed in the approach. It also proposes several options to sample the uncertainties associated to the computation of the fluxes. This will be very helpful in the development of the intercomparison project. Consequently, I just have minor suggestions for improvements.

> We thank the referee for this positive review.

I have first two small general points

1/ If I understand well, despite a relatively sophisticated approach to obtain the melt rates for present-day conditions, the warming signal simulated on the continental shelves by global climate models for future conditions is transferred without modifications into the cavities. The warming is also homogenous in the cavities, because of the extrapolation applied. If this is the case, maybe it is good to write it explicitly, for instance in the final section, to avoid misinterpretations.

> The warming signal simulated by the CMIP models is indeed transferred without modifications into the cavities, but it is not homogenous, it keeps the vertical warming profile of CMIP models and possibly regional patterns, which could produce east-west warming gradients in the largest cavities. This has been clarified as follows: "This method keeps the same vertical structure inside ice-shelf cavities as in the "ambient ocean" of observations or CMIP5 anomalies, which omits several physical processes".

2/ The computed fluxes can vary by one order of magnitude between the different parametrizations. This is a very large uncertainty and I guess this would have a major impact on ice sheet model results. I know this point is not the topic of this paper but more information on the uncertainties of those fluxes would be very helpful. Results of simulations with FESOM are suggested as a benchmark but I was wondering if other results could be included too to have a broader discussion of this important point.

> First of all, we would like to remind the reviewer that the entire paper is about the uncertainty on parameterized melt rates. This is our motivation to calculate the percentiles and to explore two very different methods to calibrate our parameters. Having said that, our range of uncertainty is indeed huge, and it is legitimate to try to reduce it. As pointed out in the review of Asay-Davis et al. (2017), so far, "few projections have been performed with ocean models including ice-shelf cavities". This statement remains

valid until now, so it is difficult to use model projections to evaluate our parameterization and possibly reduce the range of acceptable parameter values. In addition to FESOM (the only CMIP-based projection so far), we can use the study by Seroussi et al. (2017), focused on Thwaites, and in which the ocean initial and lateral-boundary conditions were uniformly warmed by +0.5°C. Applying a similar perturbation of 0.5°C to our climatology, we obtain the following results (present-day in blue vs +0.5°C in red):

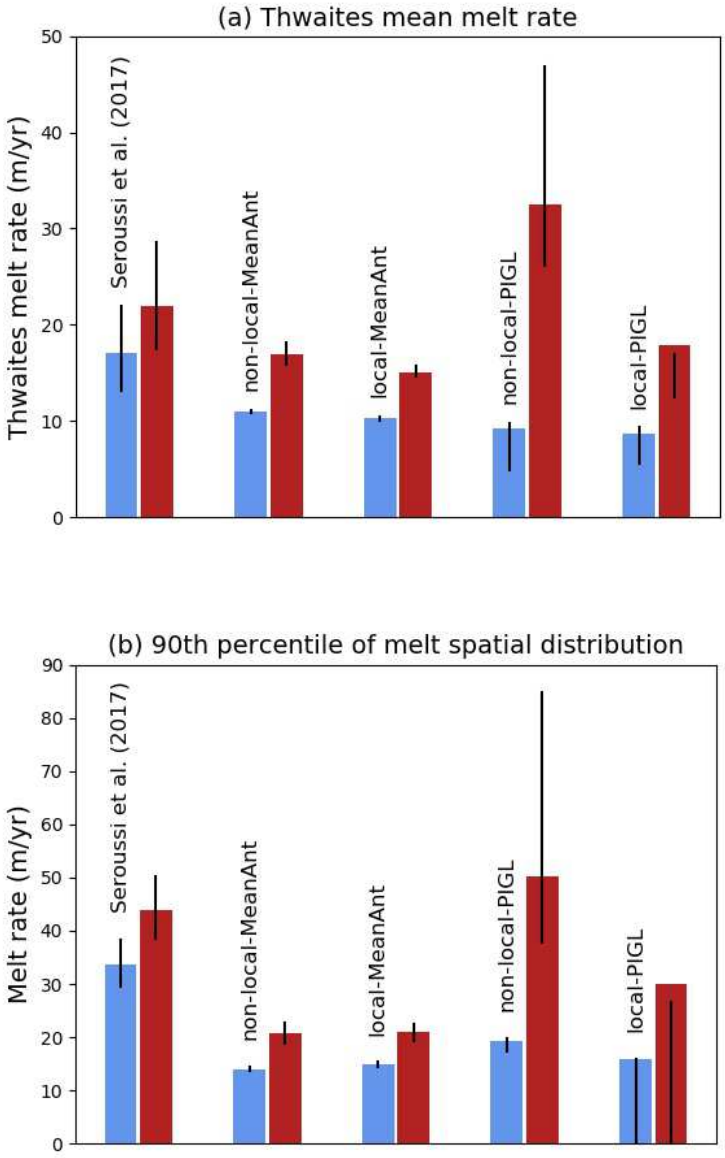

However, it is again not easy to conclude on which parameterization performs better. First of all, the present-day parameterized values are underestimated at Thwaites compared to Seroussi et al. (and to observations). MeanAnt seems in better agreement with Seroussi et al. (2017) in terms of relative increase for both average and high-end values, but "warm" (+0.5°C) non-local-PIGL melt rates are quite close to "warm" melt rates in Seroussi et al. (2017). This figure and its description have been added at the end of section 5.

Specific points

1. Page 4, lines 4-5. I do not understand what is meant by 'coupled ice sheet ocean models are not ready to be used with CMIP boundary conditions'. Is the problem that ice sheet models are not coupled to ocean models for the majority of ISMIP6 models or that those models cannot be used on the spatial-timescales of interest? I guess that, for coupled ice sheet ocean models, a protocol can also be defined to drive them by CMIP boundary conditions (but it is out of the scope of ISMIP6?) – see also page 4, line 20.

> An option for using ocean—ice-sheet coupled models was proposed in the early ISMIP6 protocol, but none of the groups was ready to run such simulations at the scale of Antarctica. So far, papers published on ocean—ice-sheet coupled models are limited to idealized configurations or regional configurations (see references in Asay-Davis et al. 2017 and Favier et al. 2019). Although some groups have started to run such global coupled models, switching to the pan-Antarctic scale and circum-polar ocean – while keeping a realistic present-day state – remains challenging. To make things clearer, we have specified "are not ready to be used with CMIP boundary conditions *at the pan-Antarctic scale*".

2. Page 8, line 17. The authors mention that the errors due to sampling, interpolation/ extrapolation are likely much larger than those due to the temporal bias. However, large interannual variability and trends have been observed in several coastal regions around Antarctica. That would thus be helpful to quantify the bias associated with the choice of the different periods, maybe using some of the data in the regions with the best coverage or using oceanic reanalyses (which have their own biases too).

> Except near a very few well-observed ice shelves (e.g. Pine Island, Dotson), there are not enough data to properly estimate the interannual variability or trends in most coastal areas. This is particularly true over the very narrow continental shelf in East Antarctica, where the inclusion of elephant-seal data decreases the temperature by more than 1°C (Fig. 1c,d). To our knowledge, there is no evidence that ocean temperature could differ by such a large amount between 1995-2017 (WOA+EN4 data) and 2004-2018 (MEOP).

About the inconsistency between the ocean data and melt rates time windows (2003-2008), we are aware about work in progress to provide interannual ice-shelf melt rates, but so far there is no interannual ice-shelf melt rate estimates published for a large majority of Antarctic ice shelves. In the case of Dotson, the average melt rate varies from 41.7 Gt/yr over 2000-2008 to 40.6 Gt/yr over 2009-2016 (the interannual peak is in 2009; Jenkins et al. 2018), so the time inconsistency between the ocean and melting datasets is likely unimportant in this case. To clarify this, we have added:

> "Estimates of interannual variability of ocean properties exist only for a handful of coastal regions around Antarctica. Based on Jenkins et al. (2018), we believe that the uncertainties due to temporal variability between these two time periods are smaller than those due to the spatial interpolation/extrapolation."

About the reviewer's suggestion to use an ocean reanalysis, there is no such reanalysis based on a model that represents ice-shelf cavities. Furthermore, existing ocean reanalyses are mostly constrained by summer

observations near the ice-sheet margins so data assimilation is unlikely to compensate the absence of ice shelves. We therefore decided not to rely on such reanalyses.

3. Page 8, line 24. The dataset proposed is different from the latest release of the World Ocean Atlas that use similar observations as input. I understand the reasons for this choice but, as many scientists will likely use this version of the World Ocean Atlas, it would be needed to highlight the main differences, for instance by showing a few maps in the supplementary material.

> Our merged dataset (WOA18p+EN4+MEOP) actually gives very similar temperatures as the latest version of WOA18's statistical mean, as shown in panel (a) below:

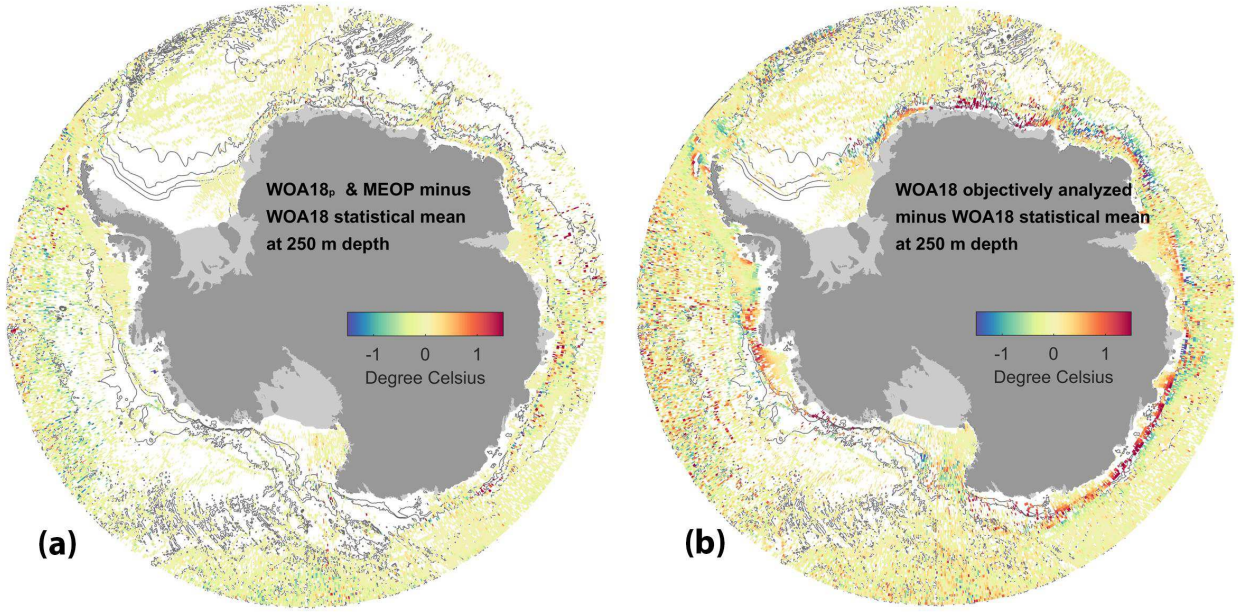

However, there are gaps in WOA18's statistical analysis, which make it impractical to constrain ice-shelf melting. It could be tempting to use WOA18's objective analysis instead of our merged dataset, but this objective analysis does not seem able to account for the strong horizontal gradients over the very narrow continental shelf of East Antarctica (see panel b). This suggests that our merged dataset may be more adequate for providing continental-shelf properties for these regions. This is now detailed in section 3 and the figure has been included as supplementary figure S1.

4. Section 4.2. Is 'thermal forcing' defined ?

> yes, it is defined in the Approach section as "the difference between the in-situ far-field ocean temperature (not modified by the buoyant plume) and the in-situ freezing temperature"

5. Page 13, line 18. The authors mention that they take samples in the melt rate and the error in the thermal forcing, using normal distributions. I may miss something but I think they take samples in the distribution of melt rate and thermal forcing (not in the error of thermal forcing). Same for Figure 3.

> The thermal forcing is different at each grid point, but we randomly add a uniform error in each sector. We do sample this error in a normal distribution, not the thermal forcing itself. We have not modified these sentences.

6. Page 13, line 30. Gamma0 is estimated by sampling the 10 highest melt rates. Would using all the melt rates for the Pine Island ice shelf lead to values that are closer to the ones obtained for the MeanAnt method?

> We have not examined this option as our aim is either to be representative of the entire ice sheet, or to get high melt rates near Pine Island's grounding line.

7. Page 15, line 9. If the temperature correction deltaT accounts for 'ocean property changes from the continental shelf to the ice shelf base' (page 12, line 12), I would assume that deltaT should be negative in most regions. Are the positive values obtained for the MeanAnt in many regions a sign that deltaT is rather compensating for a too weak exchange coefficient?

> As written in our manuscript, deltaT accounts "for biases in observational products, ocean property changes from the continental shelf to the ice shelf base (not accounted for in the aforementioned extrapolation), tidal effects and other missing physics". The PIGL calibration does create negative deltaT in most sectors. With the MeanAnt calibration, we first adjust gamma0 to get the correct melt rate for the entire ice sheet, then deltaT to get the observed melt rate in each sector. So by construction, there must be regions with positive deltaT and regions with negative deltaT. This would be one more argument to prefer PIGL over MeanAnt, but as deltaT accounts for many imperfections of our parameterization, we prefer not to over-interpret this. We have simply added this sentence when we describe the deltaT distributions:

> "We note that MeanAnt deltaT values are positive and negative by construction, while PIGL deltaT values are negative, as expected if this correction represents changes in water mass properties along the ice draft (keeping in mind that it also likely accounts for missing physics)."

8. Page 18, line 13. Is the underestimation of the melting at surface in the PIGL method a consequence of using constant deltaT on the vertical while the correction may be smaller closer to the surface?

> It depends how deltaT is interpreted. If it is seen as accounting for the water mass transformation, it should be higher in the upper layers. If it is seen as accounting for biases in the observational datasets, it should probably be higher in the thermocline. But again, many things are hidden behind deltaT, and we don't want to over-interpret this, so we have not added any comment about this.

9. Figure 6. The last but one and last but two sentences of the caption are repetitions of the second line.

> Thank you, this has been corrected.

10. Page 22, line 9. 'estimated' instead of 'reconstructed'?

> This has been modified as suggested.

11. Page 24, line 14. I would suggest ‘selected’ instead of ‘identified’ as the choice is mainly based on past results, not on new analyses performed in the manuscript.

> This has been modified as suggested.

12. Page 24. It is not clear from the discussion if the parametrization with a slope dependency is suggested or not as an option for ISMIP6.

> We have specified “While we encourage testing this parameterization, it is not part of the ISMIP6 standard protocol”.

Anonymous Referee #2

In the manuscript parameterisations and their calibration to generate basal melt rate forcing for the ISMIP6 experiments are presented. In a first step, a present-day climatology of the ocean is generated from different datasets and extrapolated by horizontal filling underneath ice-shelf and into currently ice-covered regions. The derived, local temperature and salinity then inform the parameterisations. The authors present two different parameterisations, both have a quadratic dependency on thermal forcing, one based on the local thermal forcing and one on a mixture of local and basin-wide averaged thermal forcing. Furthermore, a procedure to tune the parameters including an assessment of their uncertainties is presented. Tuning parameters are a pre-factor, which is constant for the entire continent, and basin-wide temperature corrections δT_b for 16 different basins b. The first tuning approach uses the Antarctic-wide basal mass flux for tuning of the parameters and the second approach observed melt rates close to Pine Island Glacier's grounding line. While present-day melt rates are, by construction, similar for both sets of parameters, melt rate sensitivities are very different and hence the projected melt rates differ by an order of magnitude.
In general, this manuscript is well written and presents a novel and comprehensive approach to systematic tuning of parameterisations including uncertainty ranges for parameters. It clearly indicates problems related to the tuning and potential future developments.

> We thank the referee for this positive review.

Major comments

(1) The aim of this work is to provide a suitable basal-melt rate parameterisation and oceanic input for ISMIP6 projections. Since the two calibration methods you present yield largely different results, it would be useful to identify upper and lower limits for basal melt rate sensitivities and discuss how your parameterisations fit into that range. In particular, do the projected changes in basal melt rates for the (95th percentile of the) PIGL parameterisation represents an upper limit and the (5th percentile of the) AntMean parameterisation a lower limit given current observations and modelling studies? How does the slope-dependent parameterisation fit in there?

> See our response to the 2nd general comment of Referee #1. There are very few observational data to assess the sensitivity of melt rates to changing temperature; the interannual observations at Dotson and Thwaites have been used here to evaluate the γ_0 coefficient (Fig. 8). This suggests that the PIGL method is more realistic than MeanAnt, and that the 95th percentile of PIGL's γ_0 cannot be discarded. However, comparisons to FESOM simulations (Fig. 10) or to the +0.5°C perturbation of Seroussi et al. (2017) suggest that the MeanAnt method may be more realistic, and the 5th percentile of MeanAnt's γ_0 cannot be discarded. So without obtaining more interannual observations or more model simulations (keeping in mind concerns with biases), it is difficult to narrow the range of uncertainty on γ_0.

The slope-dependent parameterization is not part of the standard ISMIP6 protocol, mostly because of calendar constraints. However, we believe that this is a promising way forward with this kind of very simple parameterization, which is why we included it in the Discussion section. As already mentioned in the Discussion "Introducing the slope dependency also strongly reduces differences between the two calibration methods (Tab. 3), thereby reducing uncertainty in projected melt rates".

(2) More details on the PIGL tuning are required, see specific comments below.

> See our responses below.

Specific comments

- page 3, line 32: I do not understand this sentence, since you only focus on basal melt rate forcing here?

> Agreed, this has been replaced with "in this paper, we focus on basal melting".

- page 5, line 19: Can such a switch be simulated in CMIP models without representing ice-shelf cavities and the continental shelf?

> Let's have a look at the conservative temperature averaged over 500-800m, averaged in a box representing the Amundsen Sea continental shelf, and for 33 CMIP5 models. Below is a scatter plot of the rcp85 warming projection (future minus present) as a function of the present-day average temperature; each character represents an individual CMIP5 model. We can see that such switches occur (e.g. models "X" and "T"), although this does not explain much of the cross-model variance. Actually, this does not necessary require an ice-shelf, it can also be related to sea-ice: if there is a lot of sea ice at present day, future warming can produce large changes in sea-ice formation and eventually stop deep convection; conversely, if there is already no much sea-ice and associated convection at present day, it will be more difficult to produce strong changes. While this is interesting, we have not added anything about this in the manuscript to keep the focus on the ISMIP6 protocol.

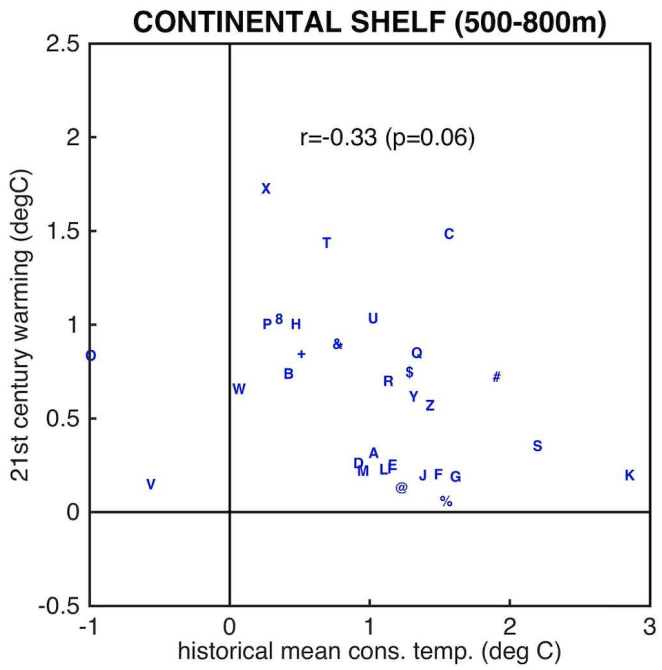

- page 6, line 28: Please explain for readers not familiar with WOA the terms `statistical mean' and `objectively analyzed mean'.

> This has been modified as:

> "We use the "statistical mean" (*average of all available values at each standard depth level in each 1° square*), rather than the "objectively analyzed mean" (*interpolation from irregularly spaced locations to a fixed grid*) values for WOA18p and EN4".

- page 6, line 30: I'm not sure I understand this, you `bin' the WOA18p data onto the same grid?

> Sorry for the confusion here. The WOA18p data are *already* binned on the WOA18p grid, so that's what we have to work with. We regrid them to the standard ISMIP6 grid before combining them with the other data sets because binning, then regridding is a lossy process that we want to try to minimize. We have modified the relevant text as follows:

> "The WOA18p data have already been binned by the creators of the dataset on the native WOA18p grid (0.25° bins in latitude and longitude). We interpolate these data (first, conservatively in the vertical and then bilinearly in the horizontal) to the ISMIP6 standard grid. Since the EN4 and MEOP data are provided at their original locations without binning, we are able to bin-average these datasets directly on the standard grid".

- page 8, line 1: Why do you use different procedures for the datasets? In particular, why do you chose to vertically interpolate the WOA18p data and not the other datasets since this might introduce vertical variations if the other data has vertical gaps?

> As explained in our previous response, the WOA18p data are already binned to a horizontal and vertical grid -- we don't have access to the original point data -- so we interpolate them to the ISMIP6 grid as best we can. Then, we combine with other datasets where we *do* have the point data on the ISMIP6 grid. Again, sorry for the misleading text that gave the impression we were doing the binning of WOA18p, rather than the creators of the dataset.

- page 8, line 22: How are salinities affected?

> The thermal forcing is not a strong function of salinity. Indeed, from 34 to 35 g/kg, the freezing point decreases by only 0.06°C. We nonetheless decided to process salinity in the same way as temperature to provide a clean dataset.

- section 3.2: Do I understand correctly that the only way the compiled observational dataset is vertically extrapolated is by filling the deeper levels with copies of the lowest available data point?

> yes, this is correct.

- page 9, line 10: `ocean model data and the climatology'

> Thank you, it is now "ocean model *and observational* data".

- page 9, line 12: Is it correct that the open ocean is not separated by the basin boundaries as shown in Fig. 2 for the interpolation (otherwise ocean regions, e.g., in the Weddell Sea, would be very small and might not contain data)? And for the ice-covered regions that the values at the boundaries are used?

> yes, this is correct.

- Figure 2, `shading' should be `colors'. Please add more explanation to the legend, especially make clear what regions are actually used in this study.

> The figure caption has been clarified.

- page 9: Please add figures showing your final datasets for an exemplary depth and along the current ice-shelf draft including basins boundaries and basin averaged values.

> The thermal forcing from the final dataset is already shown along the current ice-shelf drafts in Fig. 5, and Fig. 1c already shows temperatures of the combined dataset before extrapolation. We consider this sufficient, and have not added a figure. We have nonetheless mentioned in page 9 that "The resulting thermal forcing along the current ice-shelf drafts is shown in section 4".

- page 10, line 5: Please give an example here.

> We have added the example of Pine Island and Thwaites.

- page 13, line 8, page 15, line 5: Do I understand correctly that you fit melt rates in units of average m/a for each region, not in Gt/a? How different are results depending on the choice of average or aggregated melt rates?

> Our description was not clear, and this has been clarified. We actually fit mass loss rates (in Gt/a), not average melt rates (in m/a). This would be an important distinction if the ice shelves in BEDMAP2 (Fretwell et al. 2013; used in our study) had a different area compared to ice shelves in Rignot et al. (2013) and Depoorter et al. (2013). While there may be small differences, all these studies use observation representative of the 2000s, and should be consistent. Rignot et al. (2013) even used BEDMAP2 to map the ice thickness for a majority of ice shelves where Operation Ice Bridge did not make measurements.

- page 13, line 30: More detail is required here. In particular, do I understand correctly that you use the highest 10 melt rates from the spatial pattern? Do you fit such that melt rates in the respective location are similar, or that melt rates in the area close to the grounding line have a similar melt rate?

> This has been clarified: "we estimate gamma0 by randomly sampling one of the 10 grid points with the highest melt rates (with equal probability) and associated thermal forcing (normally distributed error) underneath Pine Island ice shelf. This is repeated 10^5 times to obtain the median, 5^{th} and 95^{th} percentiles of gamma0".

- page 15, line 2: Wouldn't it help to better constrain the melt sensitivity in PIGL by using the temporal variation from Figure 8 for calibration?

> Yes, the analysis shown in Fig. 8 came after the ISMIP6 protocol design, but this would have been an option, although it does not guarantee that melt rates are high enough near grounding lines (which was the motivation for the PIGL method).

- Figure 3 and 4: Please add explanation to the legend.

> We have added a brief explanation in these two figure captions.

- page 15, line 6: δT should represent changes of water masses being transported into the cavities as well as uncertainties in observations. Since the first would only act to decrease temperatures at depth, shouldn't a decrease in temperatures be favored over an increase (i.e., not a normal distribution be assumed)?

> As written in our manuscript, δT accounts "for biases in observational products, ocean property changes from the continental shelf to the ice shelf base (not accounted for in the aforementioned extrapolation), tidal effects and other missing physics". The PIGL calibration does create negative δT in most sectors. With the MeanAnt calibration, we first adjust γ_0 to get the correct melt rate for the entire ice sheet, then δT to get the observed melt rate in each sector. So by construction, there must be regions with positive δT and regions with negative δT. This would be one more argument to prefer PIGL over MeanAnt, but as δT accounts for many imperfections of our parameterization, we prefer not to over-interpret this. We have simply added this sentence when we describe the δT distributions:

"We note that MeanAnt δT values are positive and negative by construction, while PIGL δT values are negative, as expected if this correction represents changes in water mass properties along the ice draft (keeping in mind that it also likely accounts for missing physics)."

- page 18, line 7: If you add $\delta T = 1.07K$, how large are temperatures in the Amundsen Sea then for present day? And how do they compare to observations in that region?

> It is difficult to answer this question as our observational gridded dataset is the best estimate that we had for the climatological annual mean temperature. So in that sense, $\delta T = 1.07$ K is 1.07 K too warm compared to observational estimates. But again, δT represents more than a correction of observed temperatures, it also accounts for missing physics, which is why we did not try to overinterpret the meaning of δT values.

- page 18, line 26: Do I understand correctly, that you retune parameters here for the Amundsen region? Since changing γor δT affects the basal melt rate sensitivity, the comparison to observations is not very meaningful for the other parameter choices. Also, do you apply the observed T, S profiles as anomalies to your climatology? Such a procedure might be better to assess the parameterisations, since the melt sensitivity of your parameterisations depends also on temperature.

> We do not retune γ, which is the coefficient mostly responsible for the melt sensitivity to ocean warming, and which is actually the coefficient that we want to evaluate here. The δT value determined previously in this paper was calibrated to correct the sector-averaged thermal forcing in the non-local parameterization (so the entire Amundsen sector here). To compare to interannual observational data, we only have either Dotson or Pine Island (on different years), and we cannot calculate Amundsen-averaged thermal forcing. As such, keeping the standard δT value for the Amundsen sector does not make sense, and we choose to re-calibrate δT to match the mean observational melt rate and focus on the interannual variability. This has been clarified in Fig. 8's caption and in the associated text.

- Figure 6: Please add also uncertainty ranges based on different values of γ, similar figures for the local parameterisations as well as for the slope-dependent ones.

> Fig. 6 already contains many lines, and adding percentiles would make it difficult to read. Further, this figure is used as an illustration to explain the behaviour of our two calibration methods, and we do not think that adding percentiles would better illustrate our methodology. We have therefore kept Fig. 6 as it was.

- page 23,24: One explanation for the discrepancy could also be that with your parameterisations all ice shelves have the same melt rate sensitivity (modulated by their respective temperature), however, FRIS might have a lower sensitivity than PIG, not only due to the initial temperature, but also due to its geometric properties (see Holland et al. (2008) testing this for an idealized geometry).

> We agree, and this is the reason why we introduced the slope dependency in the Discussion section.

- page 24, line 26: It might be key to include the basal slope in parameterisation. How does this affect future changes in BMR as shown in Figure 10?

> We have added the equivalent of Fig. 10 but for the slope-dependent version (see Fig. 12 below). As already mentioned and shown in Tab. 3, the difference between PIGL and MeanAnt is reduced when the slope dependency is introduced, and the projected basal mass loss is generally much lower than with the standard ISMIP6 method.

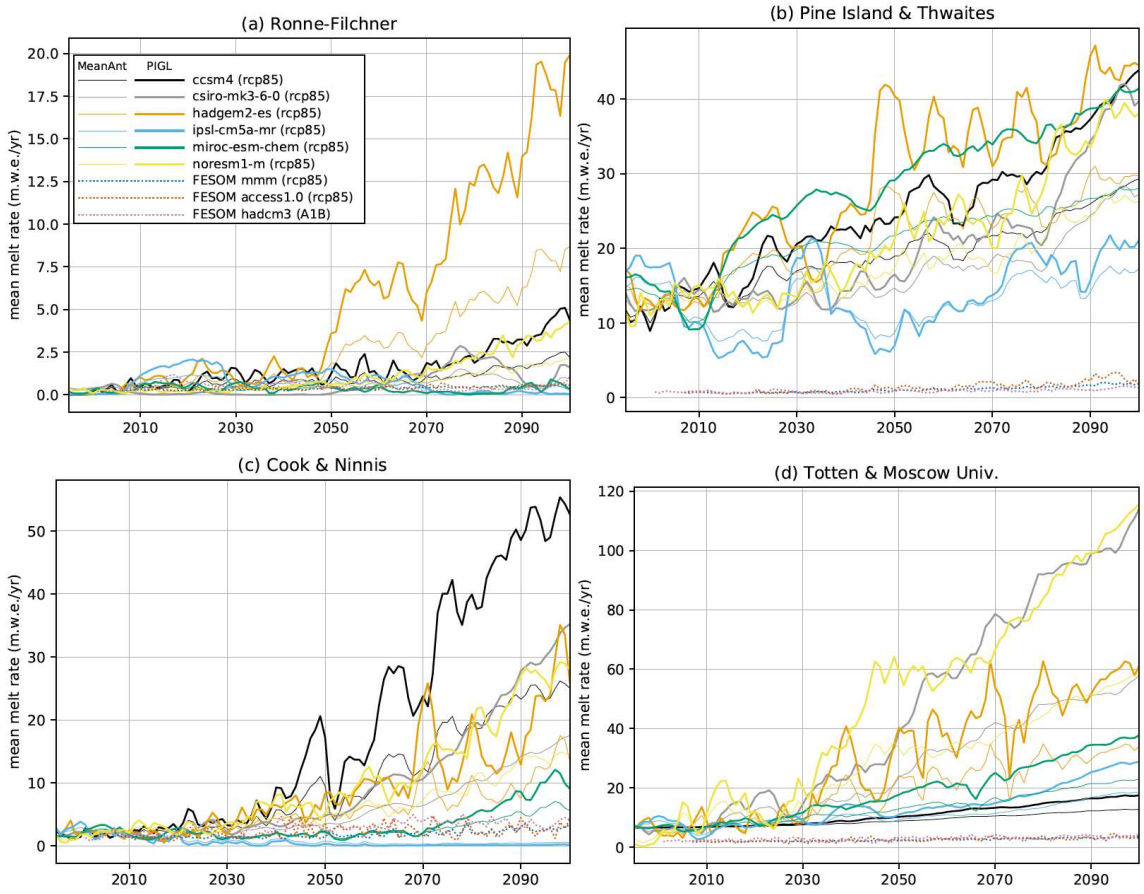

Figure 12. Same as Fig. 10, but using a slope dependency (eq. 1 multiplied by $\sin\theta$).

Hartmut Hellmer (Referee #3)

The authors present a new methodology for calculating melt rates at the base of Antarctic ice shelves to serve ISMIP6 (Ice Sheet Model Intercomparison Project for CMIP6). Based on existing observational data sets (WOA18p, EN4, and MEOP) a present-day climatology has been constructed. The evolution of ocean temperature and salinity is derived from climate models by calculating anomalies as differences between the annual means and the 1995-2014 average, then added to the present-day climatology. The proposed parameterization of basal melting depends quadratically on, due to the architecture of the ISMIP6-ice sheet models, either non-local or local thermal forcing, both constrained by the observed temperature climatology. Two calibration methods are proposed based on (1) the mean Antarctic melt rate and (2) melt rates near the deep grounding line of Pine Island Ice Shelf, the latter to cover a high melting regime expected

to become widespread in a warming climate. The still existing deficiencies of this approach ask for the consideration of more physics related to the cavity processes and more and long-term observations of hydrographic characteristics and basal melt rates.

General comments: Once having proposed a 'simple' box model to provide melt rates beneath Antarctic ice shelves and watched recent efforts with the same purpose, I highly appreciate this kind of approach based on data from ocean and ice shelf observations – though, it is just a step in the right direction and does not mark the end of the effort! My comments/questions are mostly marginal and, hopefully, will not hamper a rapid publication in TC.

> We thank Harmut Hellmer for his positive feedback.

Hartmut H. Hellmer

Specific comments (according to page and line numbers):

- P05L14: It took me a while to realize that ice shelf draft is not an issue and the open ocean profiles are extrapolated horizontally even into the ice. If I am right, please add a sub-clause for clarification.

> This is correct. We have added "and into locations currently occupied by ice".

- P08L07: I still puzzle about the procedure of extrapolating shelf water characteristics into the cavities, especially after having seen the thin lines in Figure 2. Looking at the southern Weddell Sea, one gets the impression that only a narrow band along the Filchner-Ronne Ice Shelf front has been considered, which does not even cover the most western part where High Salinity Shelf Water (HSSW), the fuel for basal melting, exists. Similar for the Ross Ice Shelf, where the most saline HSSW of McMurdo Sound is extrapolated into the cavities fringing the western Ross Sea. In addition, it is still a big unknown and its implementation technically not easy, but one should mention somewhere because of that the extrapolation into the cavities does not follow possible routes of cavity inflows.

> For the purposes of extrapolation, the basin boundaries are only used for regions of present-day grounded or floating ice, not for the open ocean. The reason we define the region in the open ocean is only because ice-sheet models will have different extent than present-day (including sometimes having calving fronts extended into present-day open ocean). In order to perform basin averages, these models need all grid points on the ISMIP6 grid to belong to one basin or another. Beyond the present-day calving front, this assignment is fairly arbitrary and probably not particularly important. Again, the extrapolation method does not use these basins.

To clarify, we have added the following text to section 3.2:

> "Note that, because we perform extrapolation first in the open ocean and then in each basin, we do not use the portions of each basin in Fig. 2 that has been extended into the open ocean. The basins have only been extended for use by ISMIP6 ice-sheet modelers, who may need the basins as part of the parameterizations described in section 4".

- P12L06: With regard to the non-local melting parameterization and the thermal forcing averaged over all ice shelves of a particular sector, one wonders how sensitive this approach is to the distribution of ice shelf drafts. I assume thermal forcing to be shifted to higher values for a sector with predominantly deep bases but this overestimates melting at lower (than average) bases.

> This is the idea behind this parameterization: in sectors with predominantly deep bases, the overall circulation induced by melting in the deepest parts of the cavities will strengthen turbulence everywhere, even along the lowest parts of ice shelf bases, as the cavity circulation is assumed to be driven by non-local processes.

- P13L06: Refreezing – obviously cannot happen for the local parameterization. Reese et al. (2018b) point to the impact of basal melting on ice flux across grounding lines, but I assume that refreezing has the same impact, at least for the big ice shelves where refreezing is widespread.

> Reese et al. (2018b) only applied mass loss, but it seems reasonable to assume that mass gain will have the opposite effect. Hence, we agree that not representing refreezing is a caveat.

- P13L17: What is the reason for using 10^5 random samples. Why not more or less?

> With 10^5 samples, the median value of γ_0 is estimated with 3 significant digits (see below), and calculations start to be extremely long for more than 10^5 samples.

1,000 samples:	$\gamma_0 = 0.1470e5$
5,000 samples:	$\gamma_0 = 0.1418e5$
10,000 samples:	$\gamma_0 = 0.1451e5$
50,000 samples:	$\gamma_0 = 0.1445e5$
100,000 samples:	$\gamma_0 = 0.1448e5$

To clarify, we have added "Using 10^5 samples gives γ_0 values that converge with 3 significant digits".

- P13L19: The uncertainty of 0.17K comes out of the blue.

> It is explained in the following sentence: "The 0.17 K uncertainty was calculated as the average temperature standard deviation at 500 m depth, between 80°S and 60°S, only considering locations with more than three valid points in the original dataset (section 3), and neglecting the uncertainty in salinity in the calculation of freezing temperature."

- P15Tab2: Some 'first-glance-surprising' results are presented without the slight attempt for an explanation. Here is an example: what is the reason for the big difference (~3 times) in the median for non-local and local PIGL?

> We have added more explanations about the PIGL γ_0 values in Tab. 2:

> "The PIGL median and 5th-percentile γ_0 values are three times higher for the non-local than for the local parameterization, which can be explained by the presence of refreezing in the first case,

requiring a large γ_0 to compensate small sector-averaged thermal forcing. For PIGL local, the 95th percentile γ_0 takes values as large as the non-local case because δT corrections become strongly negative and make the *max* function in eq. 2 produce zero melt at numerous grid points."

- P16Fig4: It took me a while to realize that the whole gray pattern (upper left) is the PIG with area of highest melt rates in red.

> We have expanded the figure caption, and this should be clearer now.

- P18L05: First, it is impossible to distinguish the different lines in Fig. 6 on a print. I had to go back to the online pdf-file to follow the writing. Second, 'good agreement' tends to be a self-serving statement, since the good agreement only holds for the depth range 400 – 1000 m, which, for FRIS, is above the depth of most grounding lines of the major ice streams.

> To improve the figure, we have thickened the lines for the future values. And we agree that "good agreement" was not appropriate. The sentence has been rewritten as "the MeanAnt method produces melt rates in good agreement with observations between 400 and 1000 m in the Ronne-Filchner sector (dashed light blue line in Fig. 6b), but underestimates melt rates at all depths in the warm cavities of the Amundsen sector by one order of magnitude (dashed red line in Fig. 6b), and in the deepest parts of Ronne-Filchner".

- P18L10. Since I cannot find any deltaT < 0 in Fig. 5c (non-local PIGL), why 'almost' everywhere?

> "almost everywhere" is for the single positive value in the PIGL-local (Fig. 5d).

A protocol for calculating basal melt rates in the ISMIP6 Antarctic ice sheet projections

Nicolas C. Jourdain[1], Xylar Asay-Davis[2], Tore Hattermann[3,4], Fiammetta Straneo[5], Helene Seroussi[6], Christopher M. Little[7], and Sophie Nowicki[8]

[1]Univ. Grenoble Alpes/CNRS/IRD/G-INP, IGE, Grenoble, France
[2]Los Alamos National Latoratory, Los Alamos, NM, USA
[3]Alfred Wegener Institute, Helmholtz Centre for Polar and Marine Research, Bremerhaven, Germany
[4]Norwegian Polar Institute, Tromsø, Norway
[5]Scripps Institution of Oceanography, University of California San Diego, La Jolla, CA, USA
[6]Jet Propulsion Laboratory, California Institute of Technology, Pasadena, CA, USA
[7]Atmospheric and Environmental Research, Inc., Lexington, Massachusetts, USA
[8]NASA GSFC, Cryospheric Sciences Branch, Greenbelt, USA

Correspondence: Nicolas C. Jourdain (nicolas.jourdain@univ-grenoble-alpes.fr)

Abstract. Climate model projections have previously been used to compute ice-shelf basal melt rates in ice-sheet models, but the strategies employed — e.g. ocean input, parameterization, calibration technique, and corrections — have varied widely and are often ad-hoc. Here, a methodology is proposed for the calculation of circum-Antarctic basal melt rates for floating ice, based on climate models, that is suitable for ISMIP6, the Ice Sheet Model Intercomparison Project for CMIP6 (6thCoupled Model Intercomparison Project). The past and future evolution of ocean temperature and salinity is derived from a climate model by estimating anomalies with respect to the modern day, which are added to an present-day climatology constructed from existing observational datasets. Temperature and salinity are extrapolated to any position potentially occupied by a simulated ice shelf. A simple formulation is proposed for a basal-melt parameterization in ISMIP6, constrained by the observed temperature climatology, with a quadratic dependency on either the non-local or local thermal forcing. Two calibration methods are proposed: 1) based on the mean Antarctic melt rate (MeanAnt) and 2) based on melt rates near Pine Island's deep grounding line (PIGL). Future Antarctic mean melt rates are an order of magnitude greater in PIGL than in MeanAnt. The PIGL calibration, and the local parameterization, result in more realistic melt rates near grounding lines. PIGL is also more consistent with observations of interannual melt rate variability underneath Pine Island and Dotson ice shelves. This work stresses the need for more physics and less calibration in the parameterizations, and for more observations of hydrographic properties and melt rates at interannual and decadal time scales.

1 Introduction

The Antarctic ice sheet has been losing mass over the last decades amounting to a net contribution to global sea-level rise of 7.6 ± 3.9 mm from 1992 to 2017 (Shepherd et al., 2018) approximately 2/3 of which occurred between 2007 and 2017 (Shepherd et al., 2018; Bamber et al., 2018; Rignot et al., 2019). About 20% of this ice loss has occurred in the Antarctic Peninsula, where the acceleration, thinning and retreat of glaciers has followed the collapse of ice shelves caused by atmospheric warming and the associated increase in surface melting (Vaughan et al., 2003; van den Broeke, 2005; Scambos et al., 2009), and possibly by decreasing sea ice cover (Massom et al., 2018). The bulk of the remaining ice loss is attributed to dynamic changes triggered by increased ocean induced melting under the ice shelves (basal melting hereafter), due to warmer ocean waters (Jacobs et al., 2011; Rintoul et al., 2016; Jenkins et al., 2018). The role of the ocean as a critical driver of ice loss is supported by numerical ice sheet simulations forced by ad-hoc basal melt perturbations that can trigger marine ice sheet instability and irreversible grounding-line retreat in West Antarctica (e.g., Favier et al., 2014; Joughin et al., 2014). The implication is that an appropriate representation of basal melting, and its future evolution, is key to projecting future ice loss from Antarctica.

In principle, these projections could be achieved through fully coupled ice sheet-ocean-atmosphere models (De Rydt and Gudmundsson, 2016; Seroussi et al., 2017). However, no such models can currently be run at a planetary scale over centuries. This is due both to the challenges presented by coupled ice sheet-ocean models and to the still poor representation of ocean dynamics along the Antarctic margins in global ocean models. Indeed, most global climate simulations that rely on ocean-atmosphere-sea ice coupled models, including those participating in the latest Coupled Model Intercomparison Project (CMIP6; Eyring et al., 2016), do not include ice-shelf cavities and therefore cannot provide projections of ocean properties beneath the ice shelves and in their vicinity (Timmermann and Goeller, 2017; Donat-Magnin et al., 2017).

A few studies have made projections based on standalone ocean models capable of representing ocean properties under ice shelves and forced by CMIP atmospheric outputs. They have shown that melt rates could increase by a factor of 2 to 3 by the end of the 21stcentury, depending on the CMIP model and ice shelf under consideration (Timmermann and Hellmer, 2013; Timmermann and Goeller, 2017; Naughten et al., 2018a). In these models, enhanced access of warm Circumpolar Deep Water to presently cooler continental shelf regions drives the largest increase in melting, but these findings vary widely across different models. Furthermore, these simulations present significant biases, in particular in the Amundsen Sea where present-day melt rates are largely underestimated (see also Naughten et al., 2018b).

Only a handful of studies have produced ice sheet projections forced by global climate simulations under various emission scenarios. Amongst these, Ritz et al. (2015) have parameterized grounding line retreat with an onset date inferred from expert judgment and standalone ocean projections (Hellmer et al., 2012; Timmermann and Hellmer, 2013), while the majority of recent ice-sheet projections have utilized basal melt parameterizations (see review by Asay-Davis et al., 2017). Although relatively complex parameterizations have recently been developed from box and plume models (Reese et al., 2018a; Lazeroms et al., 2018, 2019; Pelle et al., 2019), so far most scenario-driven ice-sheet projections have relied on simple functions of ocean temperature. These simple parameterizations are based on empirical and poorly documented choices of calibration parameters, ocean data, and the depth at which they were considered (Asay-Davis et al., 2017). Furthermore, the parameterized melt rates

are usually tuned to match observational estimates for a subset of ice shelves, and to date their response to changing ocean temperature and ice-shelf geometry has only been evaluated in a single study, in a highly idealized framework (Favier et al., 2019).

In this paper, we propose a new methodology to derive basal melt rates for Antarctic ice-sheet models from century scale climate model simulations. The methodology requires projections of ocean temperature and salinity around Antarctica which, in this effort, will be derived from CMIP models. This effort was developed as part of the Ice Sheet Model Intercomparison Project for CMIP6 (ISMIP6; Nowicki et al., 2016) aimed at providing ice sheet mass balance projections for the 6thAssessment Report of the IPCC (Intergovernmental Panel on Climate Change). ISMIP6 follows similar initiatives, such as SeaRISE (Bindschadler et al., 2013; Nowicki et al., 2013) and ice2sea (Pattyn et al., 2013; Gillet-Chaulet et al., 2012; Goelzer et al., 2013), that seek to bring together a number of ice-sheet models, and scientists from different disciplines, to better estimate the uncertainty of future ice mass loss projections from the two polar ice sheets. In contrast to other efforts targeting ice sheet-ocean coupling, ISMIP6 projections are driven offline by changes in ocean properties drawn from a subset of CMIP models. Full details of the ISMIP6 project can be found in Nowicki et al. (2016) and on the ISMIP6 webpage[1].

This paper focuses on the methodology employed to calculate basal melt rates for Antarctic ice-sheet models taking part in ISMIP6. The aim is to provide a physically based, yet technically feasible and consistent, protocol, to translate far-field ocean conditions provided by the CMIP models into a plausible range of melt rates. An important requirement is that this protocol can be utilized by ice-sheet models with a moving ice shelf-ocean interface, and that the methodology is simple enough to be used by all participating ice-sheet models. The paper is structured as follows: first, we present our approach and the rationale for our decisions (section 2); then, we present our method for obtaining the ocean thermal forcing at the base of evolving ice shelves (secion 3); next, we introduce a basal-melt parameterization and a calibration method (section 4). After this, we provide an example of present and future parameterized melt rates to illustrate our overall methodology (section 5), followed by some discussion and concluding remarks (section 6).

2 Approach

While variation in ice-shelf basal melting is not the only external forcing that can affect the Antarctic ice sheet, the loss of buttressing due to ice shelf thinning from increased basal melting, in particular of deep ice near the grounding line, is thought to be the primary driver of the increased ice discharge (e.g., Pritchard et al., 2012; Gudmundsson, 2013; Seroussi et al., 2014). Other ocean-driven changes, such as calving induced by ocean waves (MacAyeal et al., 2006; Massom et al., 2018), may also influence ice shelf stability but there is presently little evidence of their impact on long-term variations of the ice sheet mass balance. Some ice shelves may also potentially be destabilized by future atmospheric warming and subsequent snow or ice melting (van den Broeke, 2005; Scambos et al., 2009; Pollard et al., 2015) and a dedicated ISMIP6 experiment has been designed to represent these processes (Nowicki et al., in preparation). Thus, in this paper, we ~~consider basal meltingto be the only mean by which oceanic changes affect the Antaretic ice sheet~~focus on basal melting.

[1]http://www.climate-cryosphere.org/activities/targeted/ismip6

The objective of this study is to formulate a reasonable estimate of basal melting under modeled ice shelves and its variability in time, despite numerous impediments: 1) ocean properties have not been observed in most ice-shelf cavities around Antarctica; 2) CMIP Atmosphere-Ocean General Circulation Models (AOGCMs) are characterized by significant biases around Antarctica (Little and Urban, 2016) and they do not represent the ocean circulation in these cavities; and 3) coupled ice sheet-ocean models are not ready to be used with CMIP boundary conditions at the pan-Antarctic scale. This effort aims to develop an oceanic forcing that: 1) takes into account the present state of knowledge of basal melting around Antarctica; 2) can be implemented by the vast majority of ice-sheet models given the ISMIP6/IPCC-AR6 time constraints; and 3) can be derived from CMIP model output for anthropogenic emission scenarios.

The rate of melting under ice shelves is largely controlled by the properties of the ocean waters in contact with the ice and the turbulent processes that regulate the heat exchange across the ice-ocean interface (e.g., Holland and Jenkins, 1999). In all but the highest resolution models, which resolve processes down to the Kolmogorov scale, melting is parameterized by estimating the heat available for melting. This is often derived from the *in-situ* "far-field" (i.e. beneath some kind of top boundary-layer) ocean temperature, the *in-situ* freezing temperature of sea-water at a given pressure, and often the far-field ocean velocity that modulates the turbulence (Holland and Jenkins, 1999; Jenkins et al., 2010; Dansereau et al., 2014). In simple basal-melt parameterizations used in ice-sheet models, the melt rate is typically proportional to the thermal forcing: the difference between the *in-situ* far-field ocean temperature (not modified by the buoyant plume) and the *in-situ* freezing temperature. Because of the turbulence modulation by the ocean circulation, basal melt should also be proportional to the ocean velocity. Since, to first approximation, the buoyancy-driven circulation increases linearly with the thermal forcing (Jourdain et al., 2017), it follows that basal melt will be proportional to the thermal forcing squared (Holland et al., 2008).

Given that coupled ice sheet-ocean models are not ready for ISMIP6 and that CMIP models do not represent the ocean underneath ice shelves, we need to formulate melting at the base of ice shelves by using a parameterization that can take CMIP model ocean properties as an input and yield basal melt rates as an output. The most sophisticated of these parameterizations are designed to represent the ocean overturning circulation within the ice-shelf cavities, i.e. the advection of ocean heat into the cavity and the subsequent transformation of ocean properties within a meltwater plume that flows from the grounding line to the ice front along the ice-shelf base (Reese et al., 2018a; Lazeroms et al., 2018, 2019; Pelle et al., 2019). While these more complex parameterizations do capture some characteristics of observed melt rates around Antarctica, alternative parameterizations expressing melting as a simple quadratic functions of the thermal forcing, as proposed by Holland et al. (2008), have demonstrated similar skill in an idealized study (Favier et al., 2019) and are easier to implement in a large number of ice-sheet models. Therefore, in the ISMIP6 core experiments, we recommend the use of such a quadratic parameterization (see description in section 4). Given that parameterizations depend on coefficients that are not well-established, it is also important to calibrate them in a way to reproduce as well as possible present-day observational melt rates, and to obtain a meaningful sensitivity to ocean warming at the scale of Antarctica. We therefore investigate calibration methods in section 4).

Since neither the CMIP ocean models nor the simpler parameterizations account for the advection of heat and salt into cavities, or the subsequent transformation of ocean properties by the melt plume along the ice-shelf base, the implementation of this approach requires extrapolating the coastal ocean properties into ice-shelf cavities. The extrapolation is also needed

to account for future ocean water intrusions into regions which are currently occupied by ice. Unlike earlier studies which extrapolated a single ocean temperature for an entire cavity or region (e.g., the near-sea-floor temperature averaged over the nearby continental shelf, as in Cornford et al., 2015; DeConto and Pollard, 2016), here, we retain the vertical structure of the ocean temperature. This is consistent with studies indicating that the depth of the thermocline is an important control of basal melt rates (Dutrieux et al., 2014; De Rydt et al., 2014).

The resolution of CMIP models varies from a few tens to hundreds of kilometers around Antarctica, which is largely inadequate to resolve processes on the continental shelves (Stewart et al., 2018; St-Laurent et al., 2013). Furthermore, these models do not include ice-shelf cavities, or the transformation of ocean water masses by ice shelf-ocean interactions; therefore, we do not expect them to accurately represent water masses on continental shelves. There is also a relatively wide spread in the distribution of water masses simulated by the CMIP models, even in their modern-day representation (Sallée et al., 2013). Because of these considerations, the approach taken here is to use CMIP outputs to derive, for every year, a spatial distribution of anomalies in annual-mean ocean properties (temperature and salinity) around Antarctica, where anomalies are defined with respect to a common modern period for each model. These anomaly projections will then be added to a modern-day ocean climatology from observations to obtain absolute temperature and salinity to be extrapolated into the cavities and into locations currently occupied by ice.

This procedure has several advantages. It guarantees the same initial conditions for the ice-sheet model simulations and it removes model-dependent offsets. The large-scale patterns of model biases tend to remain unchanged throughout the CMIP projections (at least in the atmosphere component), even under the strongest scenario (Krinner and Flanner, 2018). This stationarity of biases suggests that it is appropriate to use anomalies, removing (by subtraction) a part of the biases in ocean projections. A caveat of this approach is that we may overestimate warming in regions that are already relatively warm, but that switch from cold to warm conditions in the CMIP models. As ice shelves act as low pass filters (Snow et al., 2017), we do not attempt to represent seasonal variability in the ocean forcing, e.g. we do not represent melting by seasonally warming Antarctic Surface Water. Because of the quadratic formulation, accounting for the seasonal variability might change the average melt rates, but we are unsure that the observational datasets can accurately represent the seasonal cycle (mostly due to the lack of observations in winter), and we leave this for future developments.

In summary, the approach used in this study involves the following steps:

- Construction, from observations, of a reasonable present-day climatology of three-dimensional temperature and salinity on the continental shelf outside of ice-shelf cavities.
- Extraction of three-dimensional CMIP temperature and salinity time series on the Antarctic continental shelf.
- Extrapolation of both the observations-based climatology and the CMIP temperature and salinity into locations with missing data, including the cavities and areas below sea level currently occupied by ice. Extrapolation is performed separately in 17 regions to prevent mixing of distinct water masses.
- Derivation of CMIP temperature and salinity anomalies with respect to the modern day to be added to the present-day observational climatology.

– Computation of the basal melting through a parameterization that takes the extrapolated ocean properties as an input.

– Calibration of the parameters used in the parameterization and assessment of the associated uncertainty.

Each step is detailed in the following sections.

For simplicity, all the fields that will be provided as part of the ISMIP6 ocean forcing are produced on a standard grid. We choose a polar stereographic grid, with a resolution of 8 km horizontally (identical to the standard ISMIP6-Antarctica grid, Seroussi et al., 2019) and 60 m vertically, which represents and acceptable compromise for ISMIP6 ice-sheet modelers between accuracy and manageable data volume.

3 Thermal forcing along the simulated ice drafts

This section describes how temperature, salinity and thermal forcing fields for the present and future are obtained inside present and future ice-shelf cavities.

3.1 Contemporary Ocean Climatology and CMIP anomalies

Constraining Antarctic coastal ocean properties is a formidable challenge, given that the Southern Ocean remains a huge data desert (Meredith, 2019). In particular the continental shelf regions are sparsely sampled, with large biases toward the sea ice free summer season. Ice-shelf cavities are even more sparsely sampled, and are not included in continental- or global-scale datasets. Therefore, observation-based products often have biases near the coast, particularly when they have been interpolated or extrapolated to fill data gaps. Ocean reanalyses and model products also have trouble properly representing coastal water masses, mostly because of scales that are not properly resolved (Naughten et al., 2018a; Nakayama et al., 2014).

Meanwhile, significant advances in hydrographic observations around the Antarctic continent have been made through the use of sensor-equipped marine mammals that yielded thousands of temperature and salinity profiles in coastal waters, including significant spatial coverage during wintertime conditions (Roquet et al., 2013). Whereas data from Argo floats, ship cruises and satellites are incorporated into most traditional ocean climatology products, observations from marine mammals were not yet included in these products at the time this project began. Fortunately, the Marine Mammals Exploring Oceans from Pole to Pole (MEOP) community had recently released a publicly available, standardized and quality controlled global dataset (Roquet et al., 2013, 2014; Treasure et al., 2017).

Thus, to obtain an improved estimate of present-day, three-dimensional fields of temperature and salinity of the coastal ocean around Antarctica, we begin by combining data from two traditional ocean climatologies, a pre-release from September 2018 of the NOAA World Ocean Atlas 2018 dataset (WOA18p; Locarnini et al., 2019; Zweng et al., 2019) and the Met Office EN4 subsurface ocean profiles (EN4, Good et al., 2013), with the complementary MEOP data. We use the "statistical mean" (average of all available values at each standard depth level in each 1°square), rather than the "objectively analyzed mean" (interpolation from irregularly spaced locations to a fixed grid) values for WOA18p and EN4 because we wanted to perform interpolation/extrapolation ourselves after combining the ~~data sets~~datasets. The WOA18p data ~~are binned~~ have already been

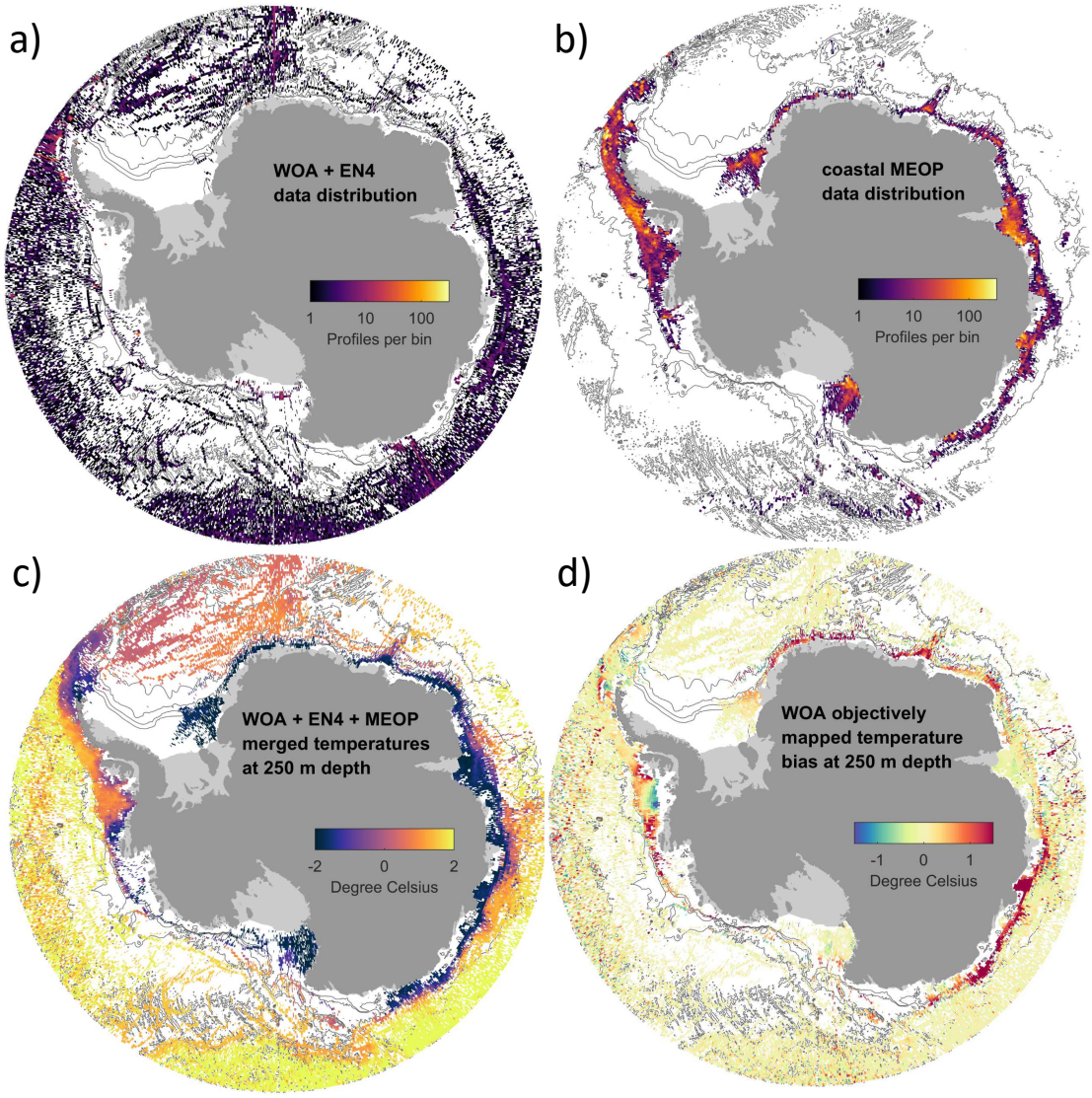

Figure 1. Circum-Antarctic coastal sub-surface data distribution counted in 0.25° bins from a) combined World Ocean Atlas 2018 pre-release (WOA18p) and EN4 ~~data sets~~datasets, b) MEOP seal profiles over areas shallower than 2500 m depth. c) These ~~data sets~~ datasets are combined to produce a sparse, merged climatological temperature dataset. d) The difference between the WOA18p objectively analyzed temperature and the merged climatology reveals biases (mostly warm) on the Antarctic continental shelf in the former.

binned by the creators of the dataset on the native WOA18p grid (0.25° bins in latitude and longitude)~~before being interpolated~~. We interpolate these data (first, conservatively in the vertical and then bilinearly in the horizontal) to the ISMIP6 standard grid. ~~Data from~~ Since the EN4 and MEOP ~~are bin-averaged~~ data are provided at their original locations without binning, we are able to bin-average these datasets directly on the standard grid. A simple average of the three datasets is then performed. Since the WOA18p and EN4 products rely to some extent on the same data source, some data sources may be double counted and have extra influence on the bin average. This is not likely to have a significant adverse affect on the results as double counting would only be a problem in areas with an abundance of data, whereas the larger problem we face is the large data gaps when we use any one of these datasets on its own. The result is a combined climatology on the standard grid that still contains significant data gaps (though less than we would have with any one of the three data sources on its own). The combined product is then interpolated/extrapolated to generate continuous fields that also extend inside the ice-shelf cavities, as described below.

We note that the temporal coverage of the ~~data sets~~ datasets differ from one another, possibly skewing the temporal coverage of the climatology toward the second half of the 23 years spanned by the three ~~data sets~~datasets. For the WOA18p and EN4 datasets, we use only data from 1995 to 2017, while the MEOP record spans 2004-2018. We further note that there is a mismatch between this time period and the 2003-2009 time frame, over which the satellite-derived basal-melt observations, used to calibrate the melt parameterization, were obtained (Rignot et al., 2013). Estimates of interannual variability of ocean properties exist only for a handful of coastal regions around Antarctica. Based on Jenkins et al. (2018), we believe that the uncertainties due to temporal variability between these two time periods are smaller than those due to the spatial interpolation/extrapolation. Additionally, due to the higher frequency of summer observations, the combined climatology likely has significant seasonal biases. However, we expect these effects to have limited influence on the decadal-scale variability of sub-surface ocean properties, which are expected to have the most influence on melt rates. The uncertainty due to large spatial gaps in observations and the resulting need for interpolation/extrapolation is likely to swamp the error resulting from any temporal bias.

Data density maps and comparisons of the merged product with objectively analyzed WOA18p fields show significant increased data coverage and reduction of bias in certain regions (Fig. 1). In particular, large parts of the narrow continental shelf region surrounding East Antarctica show a sub-surface warm bias on the order of one degree Celsius in the WOA18p data, while a similar cold bias is evident in the Bellingshausen Sea sector. Obviously, those biases will affect parameterized melt rates that largely depend on the coastal ocean temperatures. In July 2019, well after this project was underway, a final version of the World Ocean Atlas 2018 was released (Locarnini et al., 2019) that also incorporated the MEOP observations. While ~~we were not able to take advantage of this new dataset, our analysis suggests that the inclusion of MEOP data has likely improved its applicability to studies involving Antarctic coastal ocean properties .~~ the new WOA18 statistical means are close to those in our merged dataset, the objective analysis provided in WOA18 does not seem able to account for the strong horizontal gradients over the very narrow continental shelf of East Antarctica, which suggests that our merged dataset may be more adequate for providing continental-shelf properties for these regions (Fig. S1).

Besides providing a reference of contemporary Antarctic coastal ocean temperature and salinity, the climatology obtained in the above method is used when computing the projected thermal forcing based on the CMIP future model anomalies. For this purpose, CMIP potential temperatures are converted to *in-situ* temperature using the Gibbs SeaWater Oceanographic Toolbox

of TEOS-10 (McDougall and Barker, 2011). Then, temperature and salinity fields are interpolated onto the standard grid. Anomalies are calculated as the difference between CMIP annual means and the CMIP 1995-2014 average and added to the observed climatology. This general methodology can be used to obtain ocean temperature and salinity anomalies for any CMIP model under any emission scenario, while the general strategy to select the CMIP5 models used in the ISMIP6 experiments is described in Barthel et al. (2019).

3.2 Extrapolation of ocean properties into the ice-shelf cavities

The CMIP ocean model components typically include a coarse representation of the open ocean on the Antarctic continental shelf but do not explicitly resolve the circulation inside ice-shelf cavities. Basal-melt parameterizations such as those we propose for ISMIP6 require knowledge of the "ambient" ocean properties (i.e. ocean temperature and salinity unaffected by interactions with the melt plume), preferably as functions of depth within the ice-shelf cavity. In addition, bathymetric features are known to control ocean properties in ice-shelf cavities (De Rydt et al., 2014; De Rydt and Gudmundsson, 2016)—deep troughs will make it easier for warmer, deeper water masses to reach into the cavity, while sills will tend to block them. Our goal is to allow temperature and salinity fields from the observed climatology and CMIP projections to flood into the ice-shelf cavities and regions below sea level that are presently covered by glacial ice while accounting for topographic barriers.

To accomplish this, ocean model and observational data are first conservatively interpolated in the vertical to a 20-m, regular grid, then bilinearly remapped in the horizontal onto the ISMIP6 standard grid. Next, the extrapolation algorithm described below is applied first in the open ocean (outside of present-day ice-shelf cavities) and then in ice-covered regions of each of 16 independent sectors (see section 4.1 and Fig. 2). We assume that ice-shelf cavities in separate sectors will remain disconnected from one another over the timescales of ISMIP6 runs, so ocean properties are not interpolated across sectors. Note that, because we perform extrapolation first in the open ocean and then in each basin, we do not use the portions of each basin in Fig. 2 that has been extended into the open ocean. The basins have only been extended for use by ISMIP6 ice-sheet modelers, who may need the basins as part of the parameterizations described in section 4.

In each basin, and separately in each horizontal layer, we convolve the resulting fields with a 2-D Gaussian kernel with a $1-\sigma$ radius of $8\,\mathrm{km}$ to smooth the data at the grid scale and fill in missing values in open ocean. We allow this smoothing to extend the reach of the valid data by up to $12\,\mathrm{km}$. This "flooding" only applies to regions where the bedrock topography, taken from Bedmap2 (Fretwell et al., 2013), is below the depth of the layer, meaning that bathymetric sills can block access of water masses deeper than the sill. This extrapolation via Gaussian smoothing is performed repeatedly, each time extending the reach of "valid" data by an additional $12\,\mathrm{km}$, until no further cells with missing data can be reached. "Valid" data is only smoothed once in this process and is held fixed in subsequent iterations of the extrapolation process. We discovered that extrapolation by more than $\sim 12\,\mathrm{km}$ in one iteration results in unphysical mixing of qualitatively different water masses over narrow topographic features, including across the Antarctic Peninsula.

Deep ice-shelf cavities blocked by sills will not be reached by purely horizontal extrapolation, so these deeper regions are filled in by copying the *in-situ* temperature and salinity from overlying layers. Since ice-sheet models will not necessarily use the Bedmap2 topography on the ISMIP6 standard grid as we have, we also copy ocean properties vertically below the

bathymetry. This ensures that valid (and reasonable) values of ocean properties are available at all depths. To reduce the size of the final ~~data set~~dataset, we conservatively interpolate from the 20-m vertical grid to a 60-m vertical grid.

We note that, in retrospect, we should have performed vertical extrapolation (that is, copying) using *conservative* temperature rather than *in-situ* temperature because conservative temperature is the more appropriate quantity to remain constant with vertical advection. However, we estimate that this difference introduces an error in thermal forcing of no more than 0.1 K, which is certainly much smaller than other sources of uncertainty (observational errors, extrapolation, projection uncertainty, approximation error in the melt parameterization, etc.).

The extrapolation algorithm provides continuous, three-dimensional ocean fields that can be interpolated to any possible depth of the ice-shelf base for use in the basal melt parameterization of the ISMIP6 models. ~~It should be acknowledged that this simple extrapolation~~ This method keeps the same vertical structure inside ice-shelf cavities as in the "ambient ocean" of observations or CMIP5 anomalies, which omits several physical processes~~that are known to affect ocean properties inside the ice-shelf cavities~~. For example, the extrapolated "ambient" temperature inside of some of the large ice-shelf cavities (e.g. Ross and Ronne-Filchner) are typically warmer than observed temperatures, which are often below the surface freezing point as a result of the high pressure and entrainment of meltwater. These processes not represented in CMIP ocean models, which have no cavities, and there is no simple way of accounting for these in our extrapolation. Furthermore, the heat loss and freshwater input from ice shelf melting itself, the topographic steering by the ice draft topography, and the interaction of the buoyancy-driven flow in the cavity with the circulation outside of the cavity, may result in feedback mechanisms that may increase or decrease the on-shore heat transport as a response to ice shelf melting (e.g., Swingedouw et al., 2008; Hattermann and Levermann, 2010; Jourdain et al., 2017; Hellmer et al., 2017; Bronselaer et al., 2018; Hattermann, 2018). Again, there is no simple way of including these processes in this effort. Finally, poor knowledge of bathymetry beneath many ice shelves may affect the accuracy of the extrapolated ocean properties (e.g., Schaffer et al., 2016; Millan et al., 2017). The resulting thermal forcing along the current ice-shelf drafts is shown in section 4.

4 Basal melting parameterization

As explained in section 2, we suggest a relatively simple parameterization for the ISMIP6 standard experiments. The current understanding of ice-ocean interactions suggests that the total ice shelf basal melt increases quadratically as the ocean, offshore of the ice front, warms (Holland et al., 2008). However, ice-sheet models require melt rates at each location underneath ice shelves, not just the total melt rate. A first possibility is to make the melt rate proportional to the square of the local thermal forcing. Such a "local" parameterization implicitly assumes that the melt-induced circulation develops locally to reinforce turbulence and subsequent melting. However, there is evidence that the melt-induced circulation develops at the scale of the ice-shelf cavity (e.g., Jourdain et al., 2017). For this reason, Favier et al. (2019) suggested parameterizing melt rates as the product of the local thermal forcing (to keep the influence of ocean stratification) and the non-local thermal forcing (i.e. averaged over the entire ice shelf base to account for the cavity-scale melt-induced circulation). For simplicity and consistency with Favier et al. (2019), we refer to this parameterization as "non-local," although it includes a mix of local and non-local

thermal forcing. A fully non-local parameterization would be similar to that of DeConto and Pollard (2016): a single ocean temperature used to calculate the melt rates at every point of the ice shelf base.

The optimal parameterization identified for this effort is the non-local parameterization, which was found to best reproduce the results from coupled ice sheet-ocean models in an idealized context Favier et al. (2019). Because of its non-local nature, however, the implementation of this parameterization in ice-sheet models may be complicated (mostly because of parallel computations). As a result, for ice-sheet models unable to implement this non-local parameterization, the recommendation is to use the local version instead. These two basal melt parameterizations are described below. We first start by defining regional sectors used to calibrate the parameters.

4.1 Regional sectors

Given that melt rates have been estimated for more than 60 individual ice shelves (Rignot et al., 2013), we could in theory calibrate the parameterizations with different parameters in each cavity. However, ice-sheet models have evolving cavities, and their present-day ice shelves and ice flows do not necessarily correspond to the observed ones, depending on their initialization method (Seroussi et al., 2019). Furthermore, two initially distinct ice shelves may merge at some future time (e.g. Pine Island and Thwaites), leading to melt discontinuities if parameters are set at the scale of individual drainage basins. Therefore, we choose to calibrate parameters at the scale of larger sectors.

We start from the 18 sectors used in the latest IMBIE assessment (Shepherd et al., 2018) and based on drainage-basin boundaries defined from satellite ice sheet surface elevation and velocities (Mouginot et al., 2017; Rignot et al., 2019). To obtain continuous melt rates underneath all the ice shelves, we merge the two sectors feeding the Ross ice shelf, and the two sectors feeding the Ronne-Filchner ice shelf (Fig. 2). To allow simulated ice shelves to be larger than currently observed, the 16 remaining sectors are then extended into the open ocean over the full ISMIP6 standard grid by finding the basin of the closest ice-covered point to a given point in the open ocean.

4.2 Non-local quadratic melting parameterization

Melt rates in the common ISMIP6 experiments are derived using a slightly modified version of the non-local quadratic parameterization proposed by Favier et al. (2019). The parameterization is explicitly defined over regional sectors, rather than for a single ice shelf, and it includes a temperature correction:

$$m(x,y) = \gamma_0 \times \left(\frac{\rho_{sw} c_{pw}}{\rho_i L_f}\right)^2 \times (TF(x,y,z_{\text{draft}}) + \delta T_{\text{sector}}) \times |\langle TF \rangle_{\text{draft}\in\text{sector}} + \delta T_{\text{sector}}| \quad (1)$$

where $TF(x,y,z_{\text{draft}})$ is the thermal forcing at the ice-ocean interface, and $\langle TF \rangle_{\text{draft}\in\text{sector}}$ the thermal forcing averaged over all the ice-shelves of an entire sector. The uniform coefficient γ_0, with units of velocity, is somewhat similar to the exchange velocity commonly used to calculate ice-ocean heat fluxes (e.g. Holland and Jenkins, 1999; Jenkins et al., 2010). The temperature correction δT_{sector} for each sector is needed to reproduce observation-based melt rates (at the scale of a sector) from observation-based thermal forcing. The other constants are given in Tab. 1.

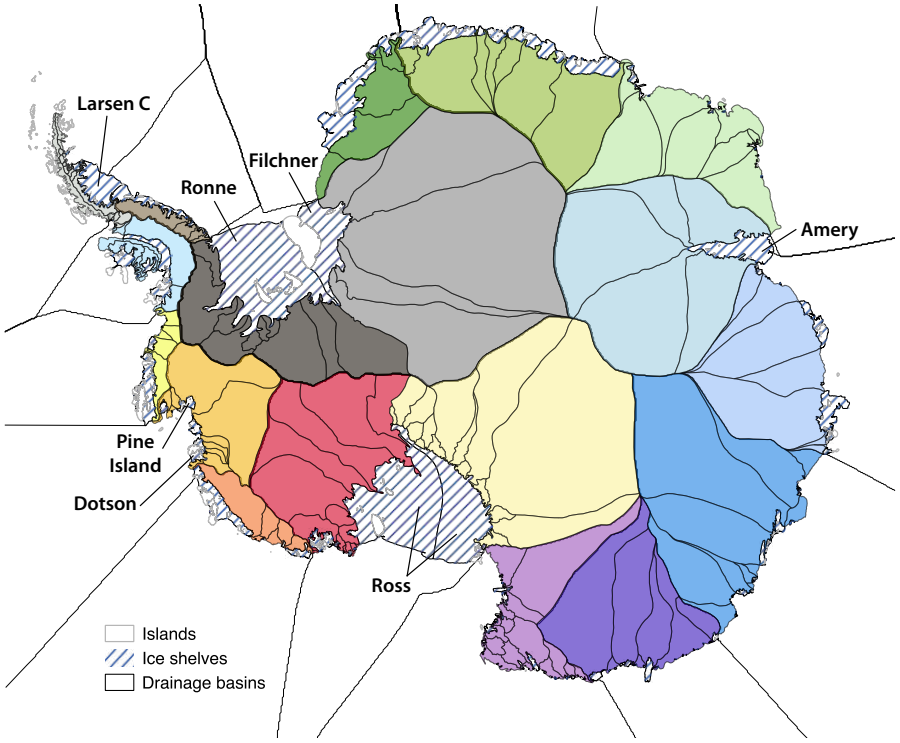

Figure 2. ~~Individual drainage basins, ice shelves, and~~ Eighteen Antarctic sectors (~~shading~~colors) defined by Mouginot et al. (2017) and Rignot et al. (2019). Individual drainage basins (black contours) are shown but are not used in this study.

The temperature correction is introduced to account for biases in observational products, ocean property changes from the continental shelf to the ice shelf base (not accounted for in the aforementioned extrapolation), ~~and tidal effects~~tidal effects, and other missing physics. A similar correction was used by Lazeroms et al. (2018). Without temperature correction, a sector-dependent γ coefficient would be required to simulate the observation-derived melt rates in each sector. This approach would lead to γ ranging from 500 to 60,000 $\mathrm{m\,yr^{-1}}$ in the different sectors, which seems difficult to justify with physical arguments. Differences across ice shelves in how efficiently available heat is converted to melting are expected, as the melt-induced circulation may respond differently to a given thermal forcing depending on its specific geometry (e.g., Jenkins, 1991; Little et al., 2009; Jourdain et al., 2017) and on regional contrasts in the amplitude of tides (Padman et al., 2018). However, tides and cavity geometry unlikely account for efficiencies across ice shelves that differ by two orders of magnitude. Furthermore, as γ explains most of the melt sensitivity to increasing thermal forcing (see eq. 1), an approach with sector-dependent γ would produce sensitivities to future ocean warming that would be strongly influenced by the regional biases in the observational products used to estimate γ. For these reasons, we think that a constant γ_0 for all of Antarctica is preferable for ISMIP6.

Table 1. Physical constants used in the melt parameterizations.

ρ_i	918.0	Ice density ($\mathrm{kg\,m^{-3}}$)
ρ_{sw}	1028.0	Sea water density ($\mathrm{kg\,m^{-3}}$)
L_f	3.34×10^5	Fusion latent heat of ice ($\mathrm{J\,kg^{-1}}$)
c_{pw}	3974.0	Specific heat of sea water ($\mathrm{J\,kg^{-1}\,K^{-1}}$)

4.3 Local quadratic melting parameterization

The non-local parameterization involves spatial integration, which may not be straightforward to implement for all the modelling groups. For those models which cannot implement the non-local parameterization, we propose a local version:

$$m(x,y) = \gamma_0 \times \left(\frac{\rho_{sw} c_{pw}}{\rho_i L_f}\right)^2 \times \{\max\left[TF(x,y,z_{\text{draft}}) + \delta T_{\text{sector}}, 0\right]\}^2 \quad (2)$$

in which the max function is preferred to the absolute value on the last term on the right in order to avoid extreme melt rates when adjusting parameters in areas with both melting and refreezing.

4.4 Calibration of γ_0 and δT_{sector} and related uncertainty

We propose two calibration methods that both provide present-day ~~sector-averaged~~ sector-integrated melt rates equal to observational estimates, but provide different melt patterns and sensitivities to ocean warming. These two calibration methods are applied to both the local and non-local parameterizations. For both methods, the calibration is done in two stages. First, it is assumed that $\delta T_{\text{sector}} = 0$ in every sector, and we estimate γ_0 based on observational constraints specific to each method, then we calibrate δT_{sector} to obtain present-day ~~sector-averaged~~ sector-integrated melt rates equal to observational estimates. For all these estimates, we use temperatures and salinity from the climatological dataset described in section 3, and the ice shelf geometry from Bedmap2 (Fretwell et al., 2013).

In the "MeanAnt" method, γ_0 is calibrated in such a way that the parameterization reproduces the total Antarctic melt rate with no thermal forcing correction, i.e. $1{,}325 \pm 175\,\mathrm{Gt\,yr^{-1}}$ (Rignot et al., 2013) or $1{,}193 \pm 163\,\mathrm{Gt\,yr^{-1}}$ (Depoorter et al., 2013), where $\pm$ indicates standard deviation. To estimate a distribution of possible γ_0 values, we take 10^5 random samples in both the total Antarctic melt rate and the error in thermal forcing, using normal distributions based on the aforementioned melt values (equally sampling Rignot and Depoorter's datasets), and assuming an uncertainty of 0.17 K for the ocean thermal forcing. ~~The later~~ Using 10^5 samples gives γ_0 values that converge with 3 significant digits. The 0.17 K uncertainty was calculated as the average temperature standard deviation at 500 m depth, between 80°S and 60°S , only considering locations with more than three valid points in the original dataset (section 3), and neglecting the uncertainty in salinity in the calculation of freezing temperature. The random error applied to the ocean thermal forcing is sampled once per sector, i.e. we assume coherent errors at the scale of a sector, and the sector random error is added to the grid-point thermal forcing. The MeanAnt method is summarized in Fig. 3.

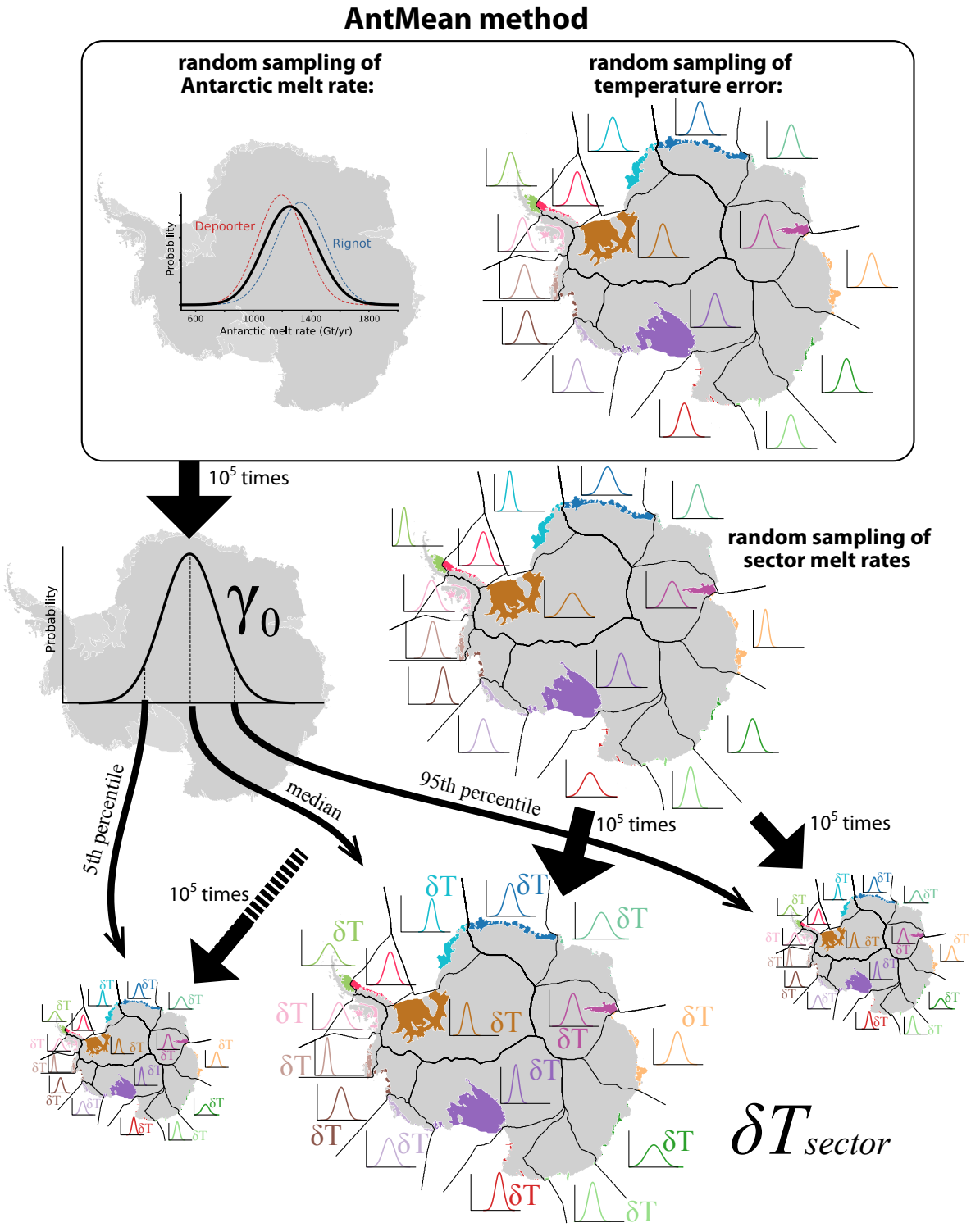

Figure 3. MeanAnt method used to calibrate γ_0 and δT_{sector}. The γ_0 coefficient is obtained from distributions of the total Antarctic ice-shelf basal mass loss and of thermal forcing with coherent normal errors in each sector (upper frame). For each resulting γ_0 value, the δT coefficients are introduced to obtain the ice-shelf basal mass loss in individual Antarctic sectors.

Table 2. Calibrated γ_0 values for the two quadratic parameterizations and the two calibration methods (in $\mathrm{m\,yr^{-1}}$).

Parameterization	Calibration	5$^{\text{th}}$perc.	median	95$^{\text{th}}$perc.
non-local	MeanAnt	9,620	14,500	21,000
local	MeanAnt	7,710	11,100	15,300
non-local	PIGL	88,000	159,000	471,000
local	PIGL	30,200	49,500	514,000

The idea behind the second method, hereafter "PIGL", is that total Antarctic melt rate may be less relevant than melt rates near deep grounding lines for ice sheet dynamics (Reese et al., 2018b). We assume that the highest melt rates of Antarctica, found near Pine Island's deep grounding line, as well as the relatively high number of ocean observations in the Amundsen Sea provide a constraint on how Antarctic melt rates could respond to strong future ocean warming. In the PIGL method, we therefore use the spatial pattern of melt rates provided by Rignot et al. (2013, here version 2.1 of their product is used) and we estimate γ_0 by ~~sampling~~ randomly sampling one of the 10 grid points with the highest melt rates ~~10^5 times~~ (with equal probability) and associated thermal forcing (normally distributed error) underneath Pine Island ice shelf. ~~The~~ This is repeated 10^5 times to obtain the median, 5$^{\text{th}}$and 95$^{\text{th}}$percentiles of γ_0. The PIGL method is summarized in Fig. 4. The values obtained through the PIGL method are an order of magnitude greater than through the MeanAnt method, and the two distributions do not overlap (Tab. 2). The PIGL ~~method is summarized in Fig. 4~~median and 5$^{\text{th}}$-percentile γ_0 values are three times higher for the non-local than for the local parameterization, which can be explained by the presence of refreezing in the first case, requiring a large γ_0 to compensate small sector-averaged thermal forcing. For PIGL local, the 95$^{\text{th}}$percentile γ_0 takes values as large as the non-local case because δT corrections become strongly negative and make the max function in eq. 2 produce zero melt at numerous grid points.

In the following, the parameterizations and calibration methods are sometimes referred to as "non-local-MeanAnt", "non-local-PIGL", and similarly for the local version.

Then, we determine δT in each sector by iterations. For each specific γ_0 value (e.g. median), we estimate δT 10^5 times by randomly sampling the ~~sector melt rates~~ sector-integrated melt rates (in $\mathrm{Gt.yr^{-1}}$) and thermal forcing in normal distributions. Random errors are sampled independently for each ice shelf within a sector when using the melt rates from Rignot et al. (2013), with a normal distribution defined by the means and standard deviations given in their Tab. 1. When using melt rates from Depoorter et al. (2013), random errors are sampled independently for each sector described in their supplementary Tab. 1. The median δT values corresponding to the median of the γ_0 distributions are shown in Fig. 5. We note that MeanAnt δT values are positive and negative by construction, while PIGL δT values are negative, as expected if this correction represents changes in water mass properties along the ice draft (keeping in mind that it also likely accounts for missing physics). Median δT values corresponding to the 5$^{\text{th}}$and 95$^{\text{th}}$percentiles of the γ_0 distributions are provided on the ISMIP6 repository (see Data Availability section).

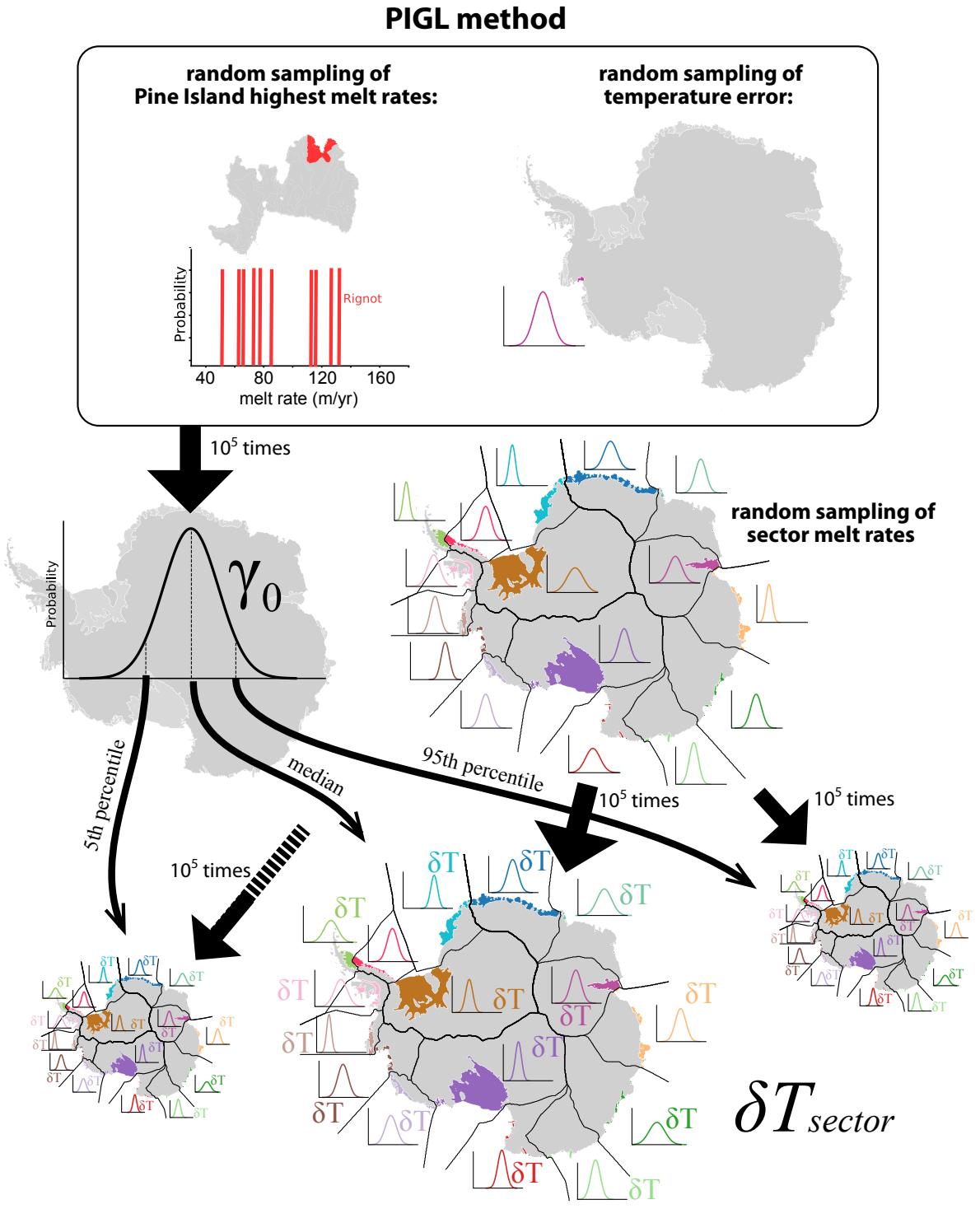

Figure 4. PIGL method used to calibrate γ_0 and δT_{sector}. The γ_0 coefficient is obtained by randomly sampling one of the 10 grid points with highest melt rates (red area in the upper left figure) beneath Pine Island ice shelf (grey area in the upper left figure), and normally distributed thermal forcing. For each resulting γ_0 value, the δT coefficients are then introduced to obtain the ice-shelf basal mass loss in individual Antarctic sectors.

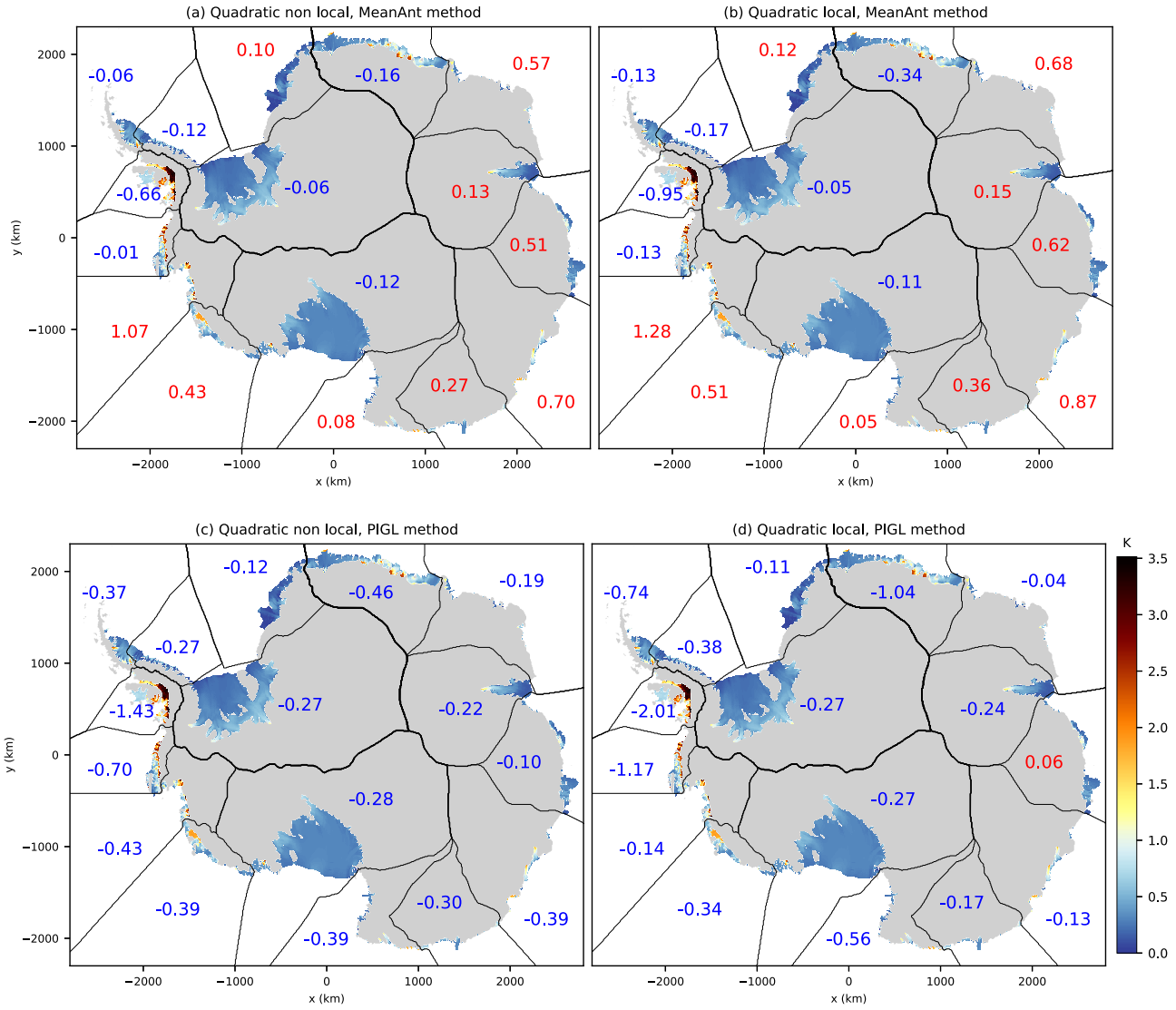

Figure 5. Thermal forcing along the ice shelf bases (shaded) and median δT corrections in each sector (numbers, negative in blue, positive in red) associated with median γ_0 estimates for the two proposed parameterizations and two calibration methods.

After this two-stage calibration, we have a distribution of γ_0 for the whole ice sheet, and distributions of δT for each sector. The ISMIP6 protocol (Nowicki et al., in preparation) explicitly requires exploration of the sensitivity of ice sheet projections to γ_0, using various γ_0 values from Tab. 2, but taking the median δT values obtained for a given value of γ_0. These experiments will thus highlight the uncertainty in the sensitivity of melting to ocean warming, but for experiments that all start from the median observed melt rates. To further explore parameter uncertainty (beyond ISMIP6 experiments), it could be interesting to randomly sample δT, independently in each sector and for each γ_0 value, to obtain a range of possible melt rates for their initial states, which would require running a much larger number of experiments to really sample the uncertainty in the different sectors.

To summarize, we suggest using either the non-local or the local quadratic parameterization in ISMIP6. For any of them, we recommend using two sets of parameters to account for the large uncertainty in parameterized melt rates: i) the MeanAnt parameters, giving a sensitivity to ocean warming based on the present-day relationship between temperatures and the mean Antarctic melt rate, and ii) the PIGL parameters, giving a sensitivity to ocean warming based on present-day high thermal forcing and melt rates near Pine Island's grounding line.

5 Results

5.1 Present-day melt rates

To illustrate the differences between the two calibration methods, we first consider the example of the non-local parameterization applied to the Ronne-Filchner and Amundsen sectors that are cold and warm, respectively (Fig. 6a). Without applying the thermal forcing correction (i.e. considering $\delta T = 0$), the MeanAnt method produces melt rates in good agreement with observations between 400 and 1000 m in the Ronne-Filchner sector (dashed light blue line in Fig. 6b), but underestimates melt rates at all depths in the warm cavities of the Amundsen sector by one order of magnitude (dashed red line in Fig. 6b), and in the deepest parts of Ronne-Filchner. Adding $\delta T = 1.07$ K brings the Amundsen Sea sector-averaged value close to the observational estimate (solid light-red line in Fig. 6b), while no substantial correction is needed for Ronne-Filchner. Without δT correction, the PIGL method fits the highest melt value of Pine Island, but overestimates melt rates in all cavities, imposing $\delta T < 0$ almost everywhere (Fig. 5). The MeanAnt method underestimates melt rates near the deepest parts of grounding lines for both the Amundsen and Ronne-Filchner sectors even after the thermal forcing correction. On the other hand, the PIGL method produces higher melt rates in the deepest parts of ice-shelf cavities, which is in better agreement with observational estimates, but yields to significantly underestimated melt rates at shallower depths (Fig. 6c).

We now assess parameterized melt rate patterns for the entire Antarctic ice sheet in comparison to the observational melt patterns from Rignot et al. (2013), as shown in Fig. 7a. The general picture is that non-local-MeanAnt produces relatively uniform melt rates within individual sectors, with maximum present-day melt rates below 25 $\mathrm{m\,yr^{-1}}$ (Fig. 7b). Non-local-PIGL produces sharper gradients, with significantly larger maximum values near grounding lines (up to 54 $\mathrm{m\,yr^{-1}}$, Fig. 7c). As in the observational product, non-local-PIGL produces refreezing areas in some sectors, but generally not at exactly the same location (e.g., Ronne, Dröning Maud Land). In the Bellingshausen Sea, areas of significant refreezing (3-4 $\mathrm{m\,yr^{-1}}$) are

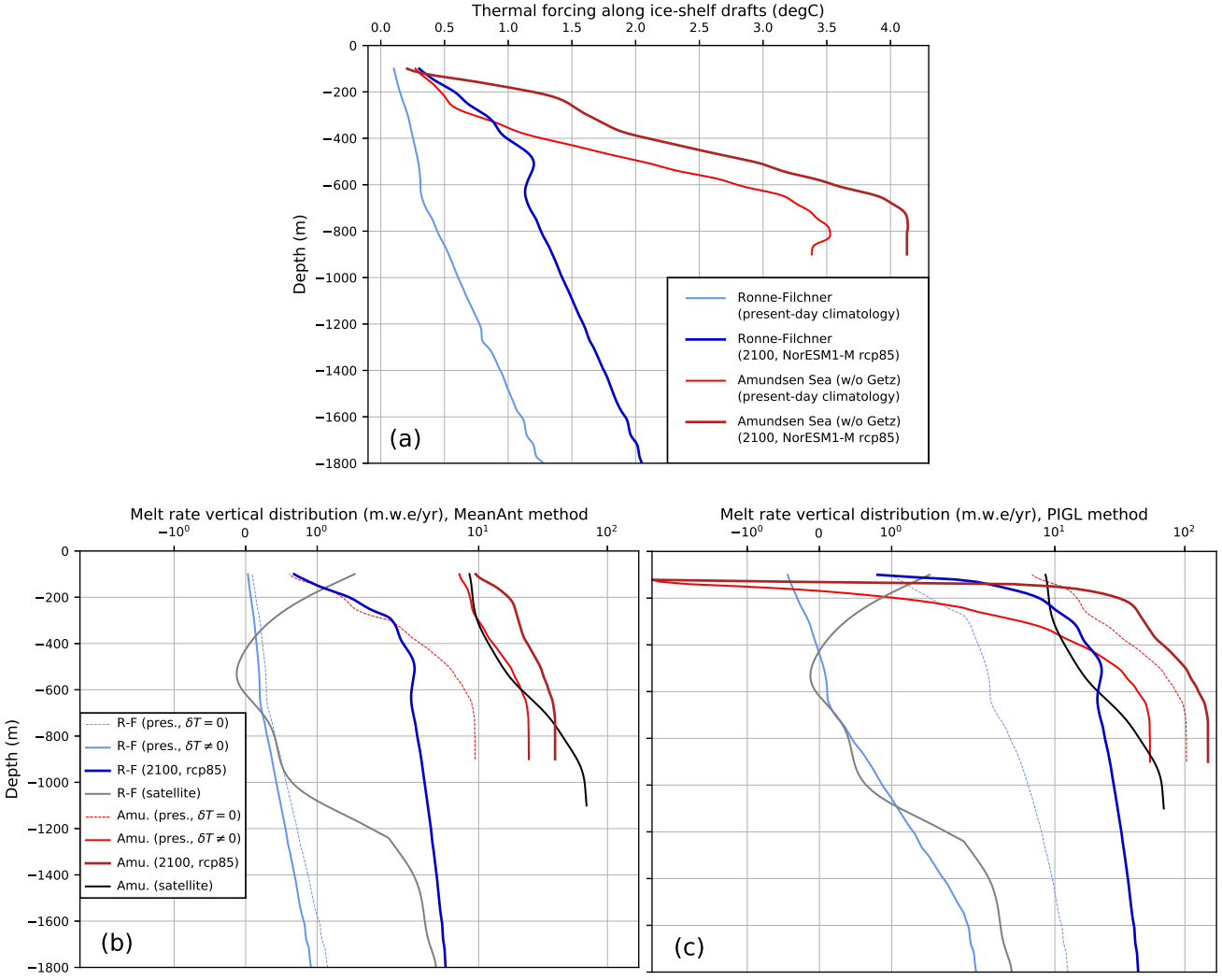

Figure 6. (a) Vertical distribution of present-day and future thermal forcing interpolated on the ice-shelf bases for the Ronne-Filchner sector (blue) and the Amundsen sector covering the ice shelves from Cosgrove to Dotson, i.e. not including Getz (red). Dark colors indicate projections. (b,c) Vertical distribution of present-day and future parameterized melt rates~~(blue and red for Ronne-Filchner and Amundsen sectors respectively)~~; the parameterized values obtained with no thermal forcing correction ($\delta T = 0$) are shown as dashed lines; ~~dark colors indicate projections;~~ the equivalent distribution for satellite-based estimates (Rignot et al., 2013, update v2.1) is shown in grey (Ronne-Filchner) and black (Amundsen). The two panels illustrate the non-local parameterization, for the two calibration methods. ~~Amundsen sector covering the ice shelves from Cosgrove to Dotson, i.e. not including Getz (red). Dark colors indicate projections.~~ The mean profiles are estimated through a Gaussian kernel density estimate.

produced by non-local-PIGL, while observations suggest no significant refreezing in that sector. The local version produces sharper gradients than the non-local, with no refreezing (by construction in eq. 2), and maximum melt rates reach 43 $\mathrm{m\,yr^{-1}}$ for the MeanAnt method (Fig. 7d) and 93 $\mathrm{m\,yr^{-1}}$ for the PIGL method (not shown) in the Amundsen Sea Sector.

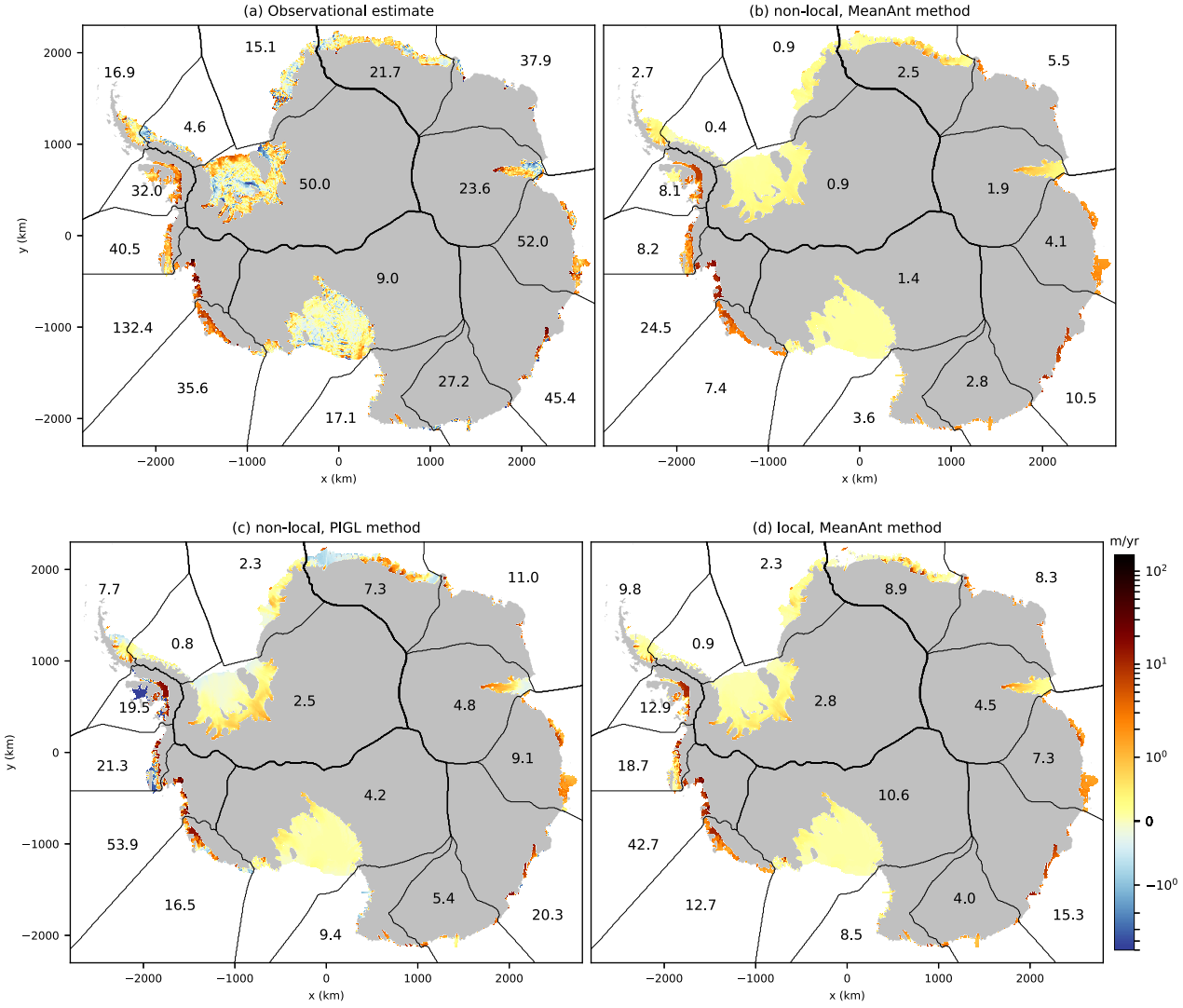

Figure 7. Present-day melt rates from (a) the observational estimate obtained by Rignot et al. (2013) (update v2.1), (b) the quadratic non-local parameterization with MeanAnt calibration method, (c) the quadratic non-local parameterization with calibration method PIGL, and (d) the quadratic local parameterization with calibration method MeanAnt. The numbers indicate maximum melt rates in individual sectors. The grounded ice sheet in shown in grey, and the black contours indicate the sectors used in this study.

While melt patterns are often used to assess basal melting parameterizations, assessing their ability to capture the interannual variability of melt rates is also valuable. The only region where both measured T,S profiles and observational estimates of

cavity melt rates are available for multiple years (thus allowing an assessment of interannual variability) is the Amundsen Sea, in particular Pine Island (Dutrieux et al., 2014) and Dotson (Jenkins et al., 2018) ice shelves. We use these T,S profiles to parameterize melt rates based on the aforementioned methods, and compare them to observational estimates (based on meltwater fluxes estimated from T,S sections under the geostrophic assumption). This comparison is used to evaluate the parameterizations themselves and the associated γ_0 that explains most of the sensitivity to ocean warming (δT values have to be adjusted differently than in the standard procedure because a single ice-shelf rather than an entire sector is observed, see caption of Fig. 8). For Pine Island, there is little agreement between the parameterized and observational variabilities, e.g. the parameterizations do not reproduce the observational peak in 2007 (Fig. 8a). In contrast, the parametrizations capture the increasing melt rate from 2000 to 2009 in Dotson, followed by a decrease and relatively stable melt rate over 2012-2016 (Fig. 8b). For both cavities, the MeanAnt method significantly underestimates the amplitude of interannual variability, while the PIGL method is close to the observational amplitude.

5.2 Example of future melt rates

Here we illustrate the ocean forcing protocol by deriving future melt rates under the Antarctic ice shelves from six CMIP5 models, considering the r1i1p1 ensemble member of CCSM4, CSIRO-mk3-6-0, HadGEM2-ES, IPSL-CM5A-MR, MIROC-ESM-CHEM, and NorESM1-M. These projections are to be considered as zero-order approximations because the depth and extent of ice shelves in the ice sheet simulations is expected to change in response to the evolving ice dynamics as well as basal and surface mass balance, which is not taken into account here. The changing geometry will be accounted for in the final ISMIP6 ice-sheet projections with all forcings combined to ice-sheet dynamics (Nowicki et al. in preparation).

As illustrated in Fig. 9 for a single CMIP5 model (NorESM1-M, Iversen et al., 2013), the mean Antarctic ice shelf melt rate can be ~~reconstructed~~ estimated throughout the historical period (1850-2005) and for rcp scenarios (2006-2100), accounting for parameter uncertainty. The early part of the historical period is close to the pre-industrial state and can be used for the long spin-up period that is sometimes needed to initialize ice-sheet models. For the NorESM1-M model, the mean melt rate remains close to the observational estimate (0.85 m.w.e/yr) under the rcp26 scenario. In contrast, the mean melt rate is strongly enhanced at the end of the 21stcentury under rcp85, reaching $\sim$6 m.w.e/yr with non-local MeanAnt and $\sim$40 m.w.e/yr with non-local PIGL (median values).

Returning to Fig. 6, we can see how the calibration method affects projected melt rates in the Ronne-Filchner and Amundsen sectors that both undergo ~ 0.75°C warming at depth: as for present-day, the PIGL method produces much stronger future melt rates at depth than the MeanAnt method (43 vs. 5 $\mathrm{m\,yr^{-1}}$ for Ronne-Filchner at 1800 m depth, and 150 vs. 39 $\mathrm{m\,yr^{-1}}$ for Pine Island at 900 m depth).

We now consider projections from six CMIP5 models under the rcp85 scenario, in four different regions where ice shelves buttress a large volume of ice grounded below sea level, here only considering the non-local parameterization (Fig. 10). For Pine Island and Thwaites, all models but IPSL-CM5A-MR indicate an increase in mean melt rate by a factor of ~ 1.5 (MeanAnt) to ~ 4.5 (PIGL) in 2100. The relative increase for the three other regions is much larger: based on PIGL parameters, a majority of CMIP5 models give projected melt rates exceeding the present-day Pine Island and Thwaites mean values ($\sim 17\ \mathrm{m\,yr^{-1}}$)

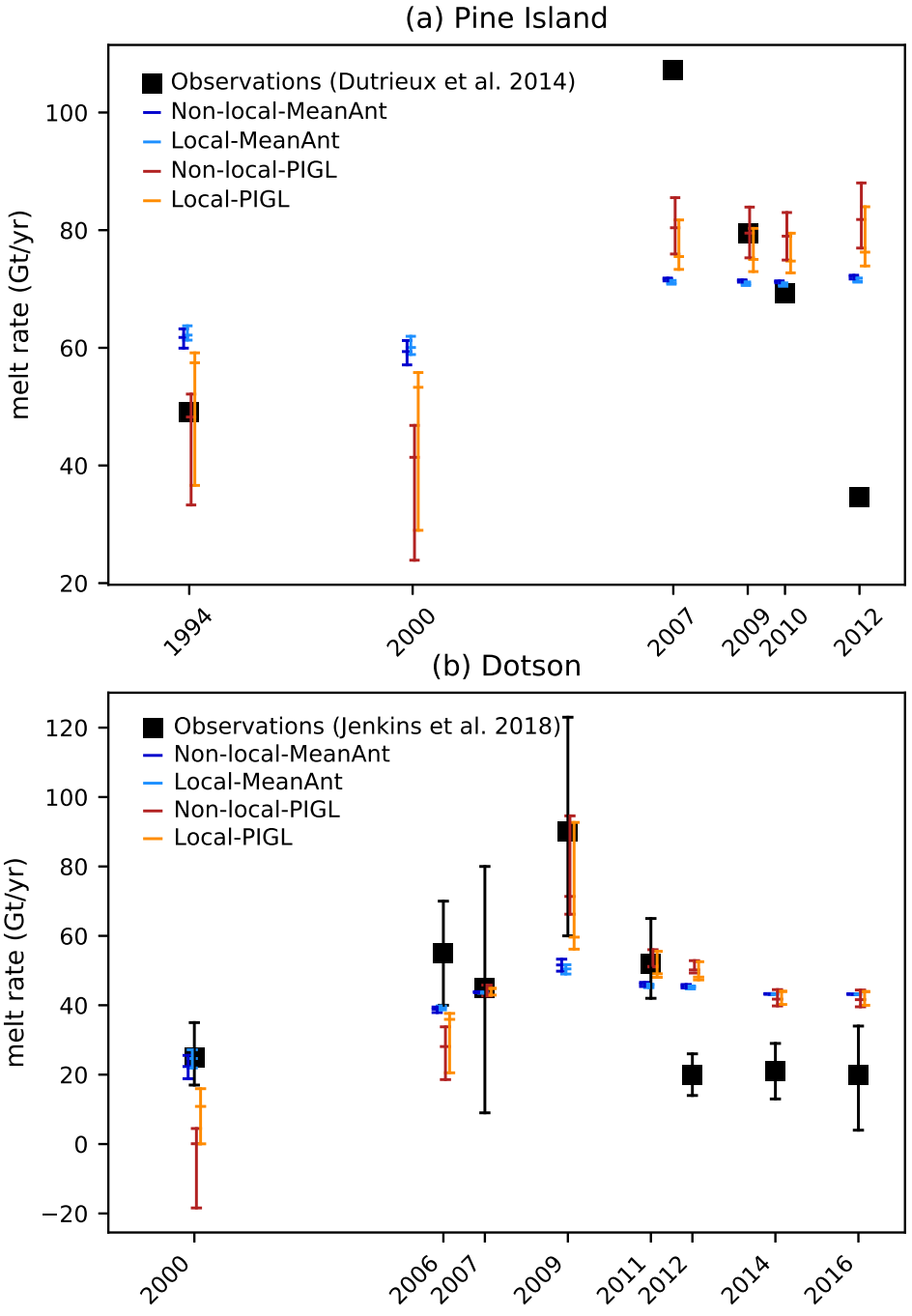

Figure 8. Interannual variability of observational and parameterized mean melt rates for (a) Pine Island and (b) Dotson cavities. Parameterized melt rates are calculated from the temperature and salinity profiles shown in Fig. 2a of Dutrieux et al. (2014) and Fig. 2a,b of Jenkins et al. (2018). For this figure, γ_0 has the standard values that are calculated for the whole Antarctic ice sheet. Keeping the δT previously determined for the Amundsen sector would not make sense as sector-averaged thermal forcing must be replaced by ice-shelf-averaged thermal forcing for this comparison. Therefore, for this plot, δT is calibrated to match the mean observational cavity melt rate, and the sector-averaged thermal forcing used in the non-local parameterizations is replaced with the cavity-averaged thermal forcing. The error bars of parameterized melt rates arise from the use of γ_0's 5th, 50thand 95thpercentiles.

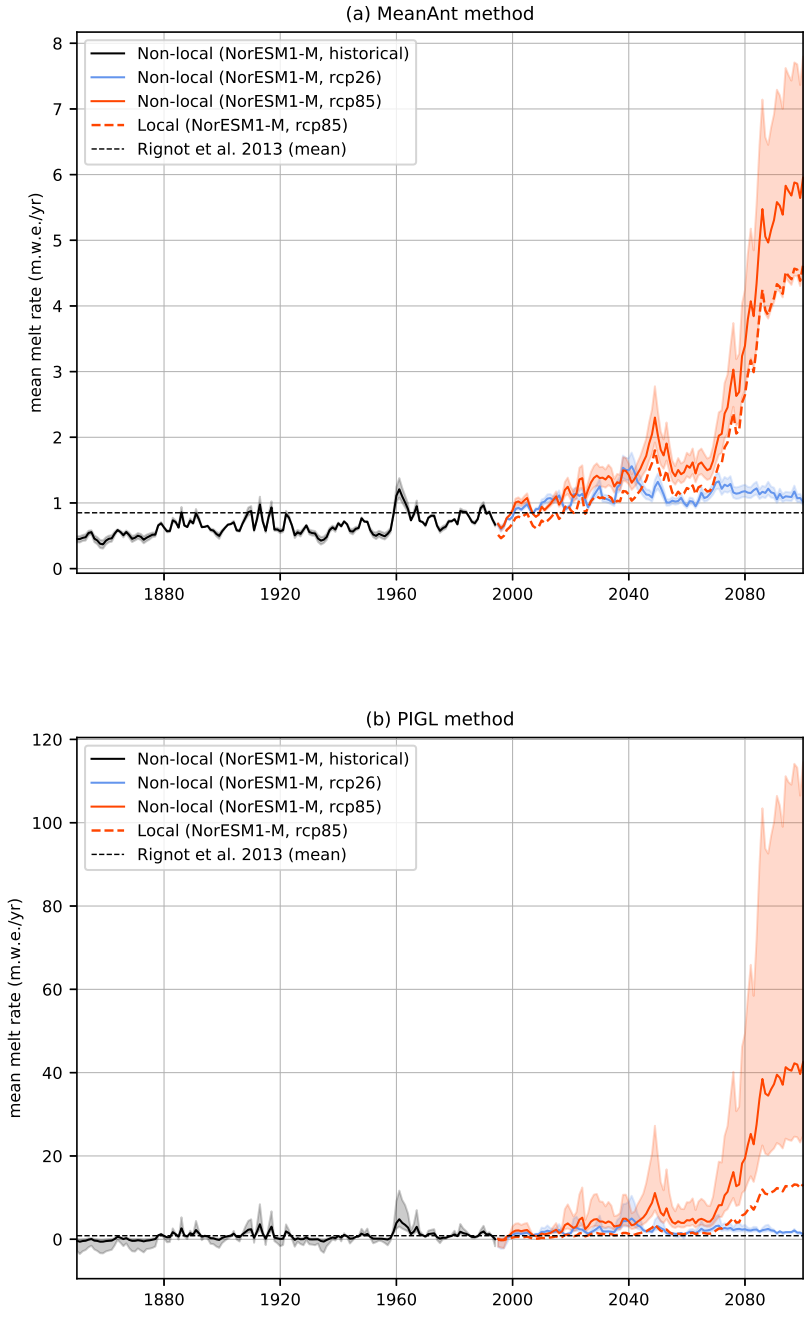

Figure 9. Time series of mean Antarctic ice-shelf basal melt rates (using the non-local parameterization and assuming a static ice-sheet geometry), based on the non-local parameterization, calibrated following (a) MeanAnt method and (b) PIGL method, and obtained from the NorESM1-M CMIP5 simulations. The semi-transparent area indicates the 5-95th percentile range related to the uncertainty in γ_0. Note the different amplitudes for the melt rates.

before 2100, even exceeding 100 $\mathrm{m\,yr^{-1}}$ for some models. The MeanAnt parameters give weaker increases for these three regions, with melt rates underneath Ronne-Filchner remaining below 3 $\mathrm{m\,yr^{-1}}$ in all models but HadGEM2-ES, and half of the models reaching ~ 10 $\mathrm{m\,yr^{-1}}$ underneath Cook and Ninnis and ~ 20 $\mathrm{m\,yr^{-1}}$ underneath Totten and Moscow University by 2100.

Comparing these results to projections from ocean models that represent ice-shelf cavities can be used to assess projections from the proposed parameterizations. Such model projections were done for CMIP3 and CMIP5 models by Timmermann and Hellmer (2013) and Naughten et al. (2018a), respectively, using the FESOM ocean model. The FESOM simulations produce realistic present-day melt rates beneath Ronne-Filchner, and their projected melt rates are close the low end of the CMIP5 distribution for non-local-MeanAnt. By contrast, half of the CMIP5 models used through non-local-PIGL give melt rates above 20 $\mathrm{m\,yr^{-1}}$, which is much above FESOM projections to 2100 (Fig. 10a), and still much above the 6 $\mathrm{m\,yr^{-1}}$ in 2200 under much warmer conditions (Timmermann and Hellmer, 2013). This could suggest that our melting parameterization is too sensitive to warming (overestimated γ_0), although this is not what is suggested by our previous analysis of Dotson and Pine Island interannual vairiability (Fig. 8). Alternatively, it could mean that projected ocean warming is largely overestimated by some CMIP5 models in the Weddell Sea.

In contrast to Ronne-Filchner, present-day melt rates produced by FESOM were significantly underestimated in other cavities, as reported by Timmermann and Hellmer (2013) and Naughten et al. (2018a). For example, the underestimation reached a factor of 10 beneath Pine Island and Thwaites, as well as beneath Totten and Moscow University (see dotted lines in Fig. 10), mostly due to overly strong convection and to the subsequent presence of cold water in these regions as discussed by Naughten et al. (2018b, a). These strong present-day biases make it difficult to use these ocean simulations as a reference to assess projections from the proposed parameterizations.

FESOM is the only model so far that has been used to build CMIP-based projection of ice-shelf melting. Seroussi et al. (2017) have run more idealized projections, adding $+0.5$°C to the initial state and lateral boundary conditions of a regional ocean simulation centered on the Eastern Amundsen Sea. We use their simulation to evaluate the sensitivity of melt rates to warming beneath Thwaites glacier (Fig. 11). It is again not easy to conclude on which parameterization performs better. First of all, the present-day parameterized values are underestimated compared to Seroussi et al. (2017) (and to observations). MeanAnt seems in better agreement with Seroussi et al. (2017) in terms of relative increase for both average and high-end values, but the warm state of non-local-PIGL is quite close to the warm state in Seroussi et al. (2017).

6 Discussion and Conclusion

In this paper, we have combined three available datasets (MEOP, WOA18 pre-release, EN4) to provide reasonable present-day ocean properties along the Antarctic ice sheet margins. These data, as well as future-present anomalies from CMIP models, have been regridded onto a common grid and extrapolated to any location that may be occupied by ocean waters in ice-sheet model projections. We have then ~~identified~~ selected a quadratic formulation as an optimal choice to parameterize basal melting in ISMIP6 Antarctic projections, following either a non-local or a local formulation. The calibration of these parameterizations

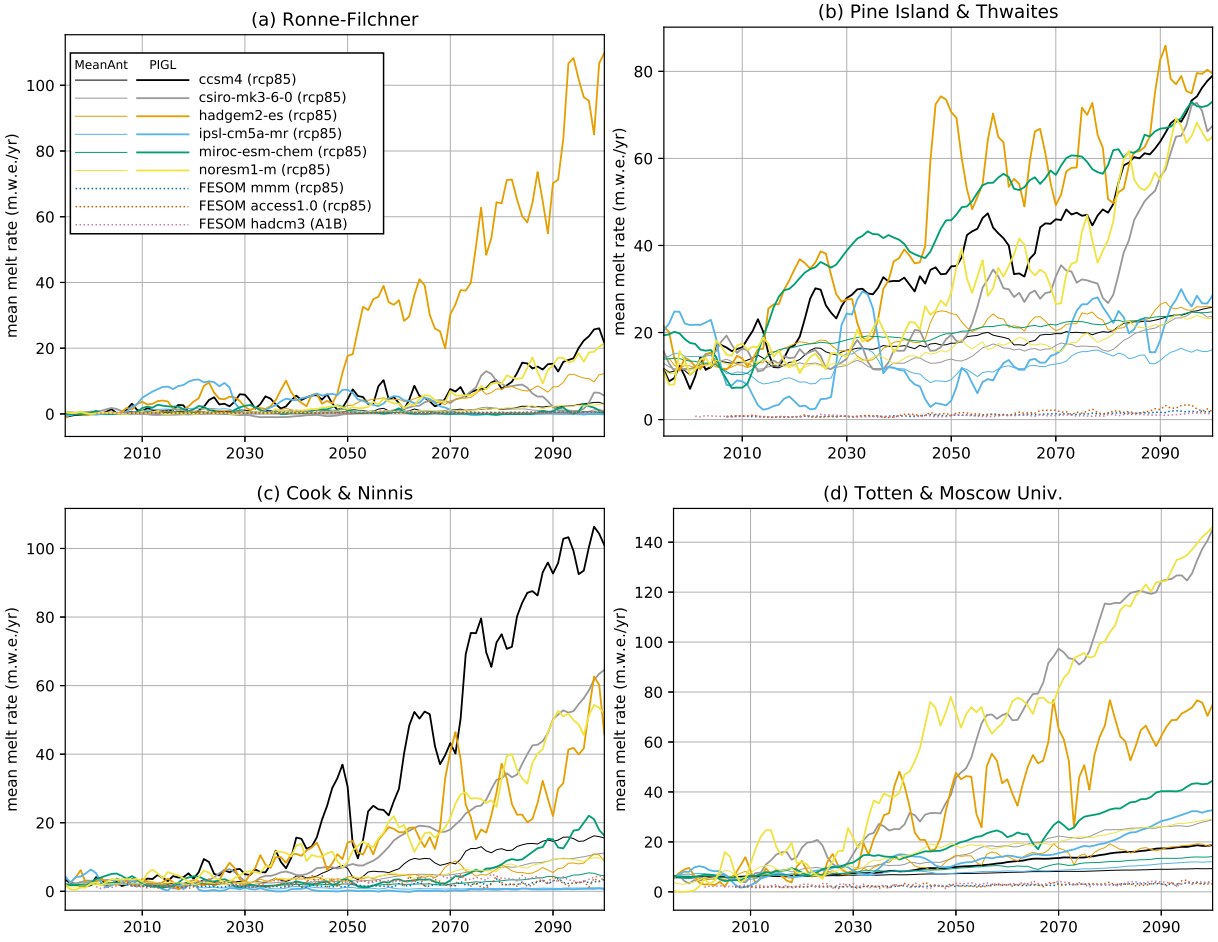

Figure 10. Time series of mean cavity basal melt rates over the 21st century under the rcp85 scenario for (a) Filchner-Ronne, (b) Pine Island and Thwaites, (c) Cook and Ninnis, and (d) Totten and Moscow University. The projection is shown for six CMIP5 models with both the MeanAnt (thin lines) and PIGL (thick lines) calibrations. The average over 1995-2014 corresponds to the observational estimates. Three projections from the FESOM ocean model (resolving ice-shelf cavities) are included; they are forced by atmospheric fields from either the ACCESS-1.0 or the CMIP5 multi-model mean (MMM) as described by Naughten et al. (2018a), of from the CMIP3 HadCM3 model as described by Timmermann and Hellmer (2013).

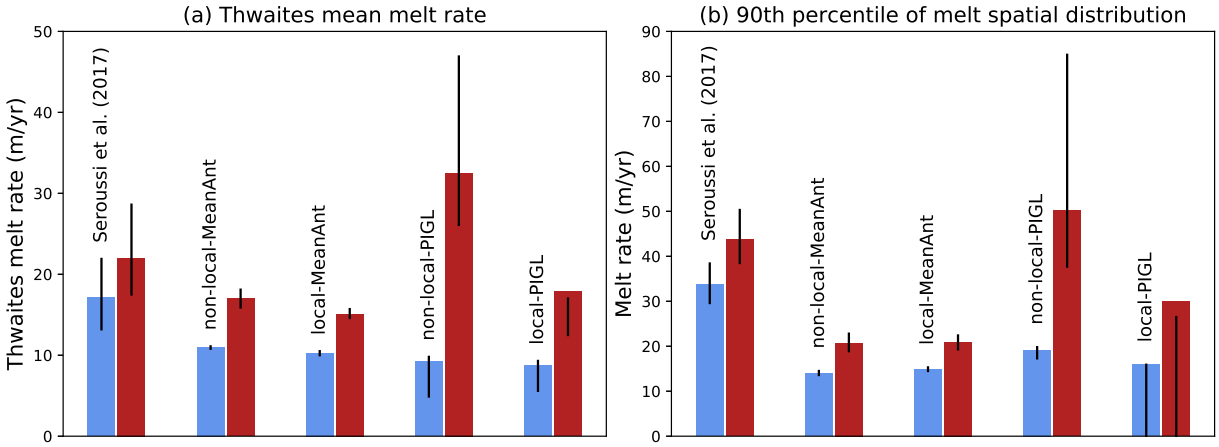

Figure 11. (a) mean basal melt rate beneath Thwaites at present day (blue) and with a $+0.5^{\circ}$C anomaly (dark red), as simulated over the first 20 years of Seroussi et al. (2017)'s simulation, and as parameterized through the ISMIP6 protocol. (b) same as (a), but showing the 90$^{\text{th}}$percentile of the melt spacial distribution. The diagram is obtained with median γ_0, and the black bars indicate values obtained with 5$^{\text{th}}$and 95$^{\text{th}}$percentiles of γ_0. Note that the 90$^{\text{th}}$percentile of the melt spacial distribution can be zero due to the max function used in the local parameterization.

determines to a large extent future basal melt rates in a given CMIP projection, and we have proposed two calibration methods to represent the related uncertainty in ISMIP6 projections, the first one calibrated globally using mean Antarctic melt rate estimates and second one calibrated with the highest melt rates estimated today in a region where direct observations of ocean conditions are available (Pine Island). In the examples analyzed in this paper, there is typically an order of magnitude difference between the lower and upper estimates of melt rates at the end of the 21$^{\text{st}}$century.

The simple approach of this paper was chosen to facilitate implementation in the wide range of ice-sheet models participating in ISMIP6. More complex formulations (e.g. Reese et al., 2018a; Lazeroms et al., 2018; Pelle et al., 2019) involve calculating distances and ice draft slopes, which may not be straightforward for all groups given the short time constraints of ISMIP6 and IPCC-AR6. However, using parameterizations that were derived from analytical physical expressions (e.g., Lazeroms et al., 2019) would make them less dependent on empirical calibration methods and should therefore be encouraged for future ice-sheet projections, although further evaluation will also be required. There are also ways to slightly increase the complexity of our approach, for example by including a dependency to the local slope in our simple formulations (eq. 1 multiplied by $\sin\theta$), as suggested by Little et al. (2009) and Jenkins et al. (2018). Applied to non-local-MeanAnt, this method produces much more realistic melt rates near grounding lines (Fig. 12b), with smaller thermal forcing corrections (Fig. 12a) than without slope dependency (Fig. 5). Introducing the slope dependency also strongly reduces differences between the two calibration methods (Tab. 3), thereby reducing uncertainty in projected melt rates ~~.~~(Fig. 13). Interestingly, the ice-shelf basal mass loss from the slope dependent version of PIGL is generally significantly lower than from the standard PIGL method (Fig. 13). This parameterization would nonetheless need to be evaluated through an ice sheet model, in a similar way as Favier et al. (2019),

Table 3. Calibrated γ_0 values (in $\mathrm{m\,yr^{-1}}$) for the quadratic non-local parameterization including a dependency to the local slope (eq. 1 multiplied by $\sin\theta$).

Parameterization	Calibration	5$^{\text{th}}$percentile	median	95$^{\text{th}}$percentile
non-local (slope)	MeanAnt	1.47×10^6	2.06×10^6	2.84×10^6
non-local (slope)	PIGL	~~0.86~~ 2.93 $\times 10^6$	~~1.59~~ 5.36 $\times 10^6$	~~4.67 $\times 10^6$~~ 2.94 $\times 10^7$

to make sure that the slope dependency does not produce unstable behaviours and that the temperature-dependency is well represented. While we encourage testing this parameterization, it is not part of the ISMIP6 standard protocol.

The assessment of basal melting parameterizations is strongly limited by the lack of observational temperature and salinity profiles as well as meltwater fluxes at interannual and decadal time scales. The only places where such assessment is possible are Pine Island and Dotson ice shelves. We have shown that the proposed parameterizations reproduce the general behaviour of interannual melt variations for Dotson but not for Pine Island. The calibration method based on the highest melt rates near Pine Island's grounding line (PIGL) produces a range of melt values closer to observational estimates than the alternative method (MeanAnt). Nonetheless, such an assessment remains limited to small warm cavities. In contrast, the MeanAnt parameters give melt rates that are in better agreement with FESOM ice shelf-ocean projections, at least for Ronne-Filchner. Large present-day biases for warm cavities in FESOM make it useless to assess projections in these environments. It should also be noted that cavity-averaged melt rates are not what ice-sheet models are most sensitive to, and melt rates near grounding lines are more relevant (e.g., Reese et al., 2018b).

Beyond the parameterization itself, another limitation of the ISMIP6 ocean forcing is the use of CMIP models to provide the regional ocean warming signal. Indeed, the CMIP models have important biases in the Southern Ocean region in terms of sea ice cover (Turner et al., 2013), westerly winds (Bracegirdle et al., 2013), and ocean temperatures (Little and Urban, 2016; Barthel et al., 2019). These biases likely affect the ice shelf melt projections, even if our anomaly approach is expected to remove a part of the mean state biases. There are also structural errors in the CMIP models, notably their coarse resolution, which prevents representation of important processes on the Antarctic continental shelf, and the absence of feedbacks between freshwater released through ice-shelf and iceberg melting and the ocean components of CMIP models. Recent studies suggested that the ocean subsurface may warm by a few tenths of a degree by 2100 in response to large freshwater released by the Antarctic Ice Sheet (Bronselaer et al., 2018; Golledge et al., 2019; Schloesser et al., 2019). There are also more local feedbacks that are not represented in our framework. For example, increased ice-shelf melting can lead to more advection of offshore circumpolar deep water towards the grounding lines and thereby create a positive feedback to melt rates (Hellmer et al., 2017; Timmermann and Goeller, 2017; Donat-Magnin et al., 2017).

All these feedbacks and the difficulty in parameterizing melt rates clearly point towards ice sheet-ocean coupling as the best way forward for centennial simulations such as ISMIP6. Ideally, ice-sheet models would be embedded in the ocean-atmosphere coupled system. However, resolving the ocean circulation in ice-shelf cavities at the resolution required to capture all these processes is costly, and so far not possible for millennial or large-ensemble simulations. Hence, parameterizations will remain

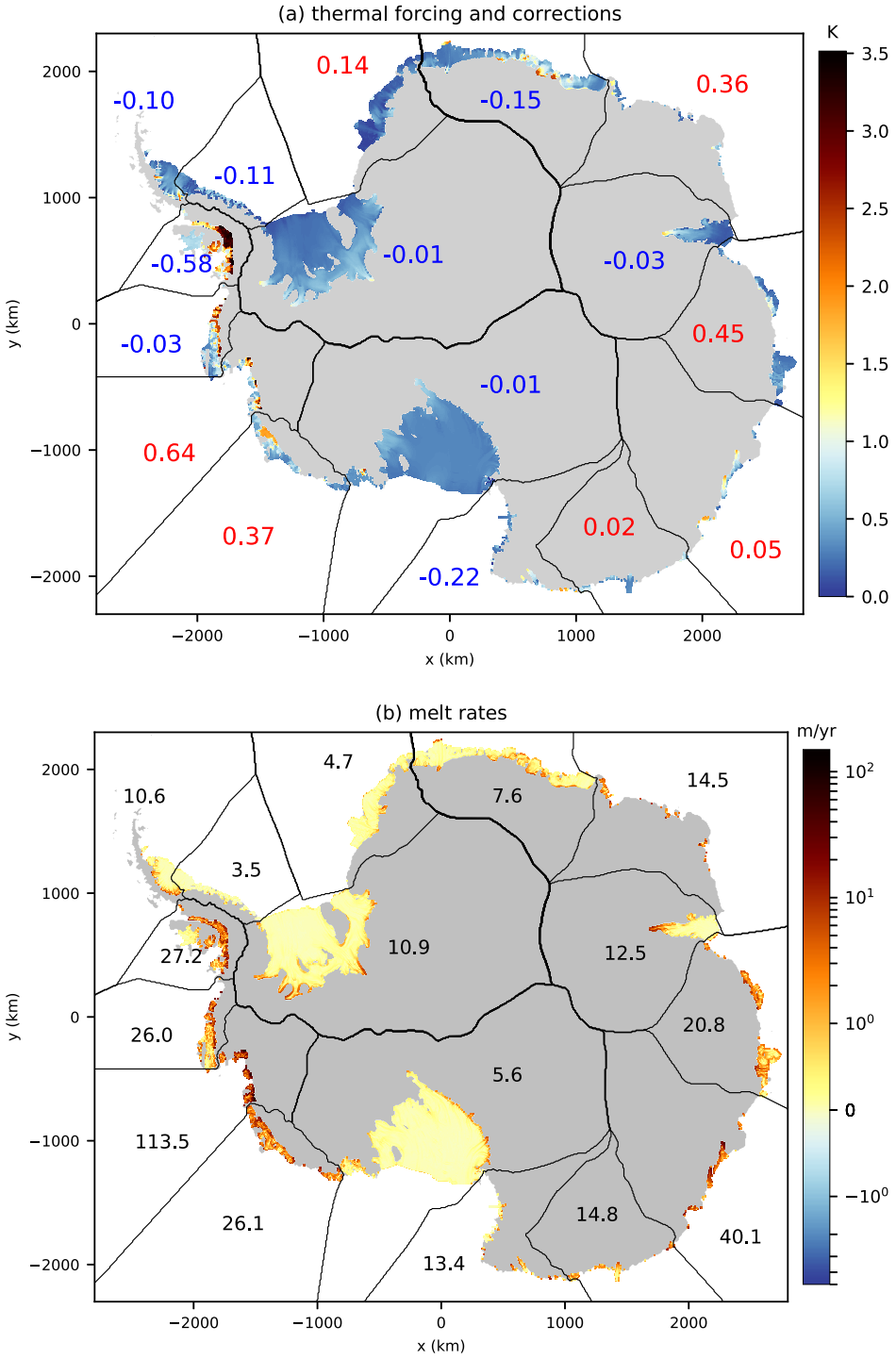

Figure 12. (a) Thermal forcing (shaded) and its corrections (blue/red numbers indicating negative/positive δT) applied to each sector for non-local-MeanAnt with a slope dependency (eq. 1 multiplied by $\sin\theta$). (b) Present-day melt rates for non-local-MeanAnt with a slope dependency. Black numbers indicate melt maxima in individual sectors.

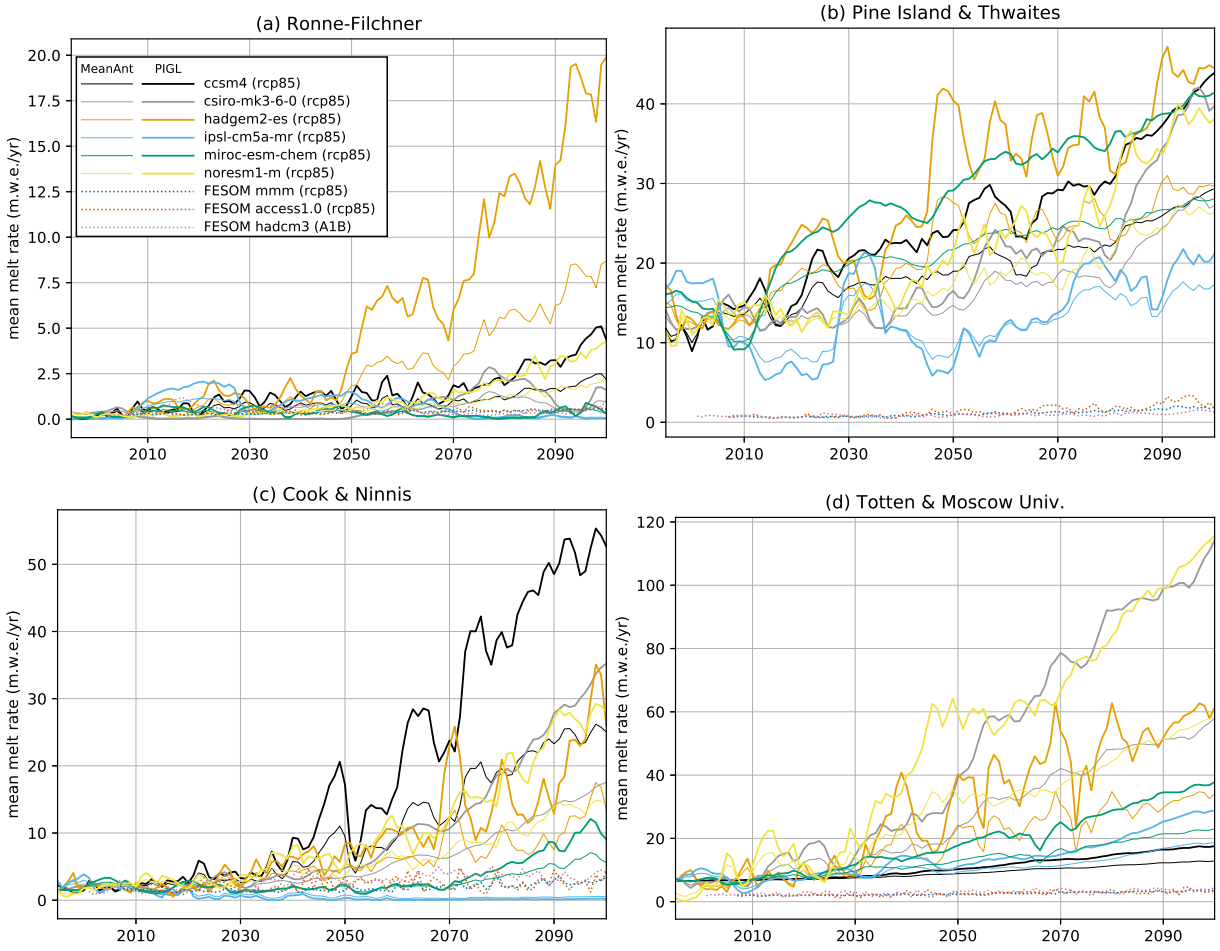

Figure 13. Same as Fig. 10, but using a slope dependency (eq. 1 multiplied by $\sin\theta$).

critical, and more work will be needed to assess (i) their ability to reproduce observed melt patterns, (ii) their sensitivity to changing ocean temperature, and (iii) their sensitivity to changing ice draft (slope, size).

Code availability. The tools used in this paper to prepare observational and CMIP5 ocean properties, and to calibrate the parameterizations, are available on https://github.com/ismip/ismip6-antarctic-ocean-forcing.

Data availability. All of the projection dataset described in this paper are freely available from the ISMIP6 ftp server hosted at the University at Buffalo; access can be obtained by emailing ismip6@gmail.com. The dataset will also be made available via the CMIP6 archive at the same time as the ISMIP6 ice sheet model simulations.

Author contributions. TH and XAD prepared the observational ocean dataset. XAD developed the extrapolation method and prepared the CMIP5 data. NJ developed the calibration methods and calculated present and future melt rates. HS made preliminary ice sheet simulations to test the proposed strategy. FS led the general effort to build the ISMIP6 ocean forcing, while SN led the ISMIP6 effort. NJ, TH and FS wrote the initial draft. All authors actively contributed to the choices that are proposed in this paper, and all contributed to the manuscript.

Competing interests. Helene Seroussi and Sophie Nowicki are editors of the ISMIP6 special issue of The Cryosphere. The authors declare that no other competing interests are present.

Acknowledgements. We thank both Adrian Jenkins and Bill Lipscomb for suggesting that we account for the ice base slope as shown in Fig. 12. We thank Pierre Dutrieux for suggesting to evaluate the interannual variability of Dotson and Pine Island as shown in Fig. 8. We thank Ralph Timmermann and Kaitlin Naughten for providing their FESOM simulations and for useful discussions. NJ is funded by the French National Research Agency (ANR) through the TROIS-AS project (ANR-15-CE01-0005-01) and by the European Commission through the TiPACCs project (grant 820575, call H2020-LC-CLA-2018-2). Support for XAD was provided through the Scientific Discovery through Advanced Computing (SciDAC) program funded by the US Department of Energy (DOE), Office of Science, Advanced Scientific Computing Research and Biological and Environmental Research Programs. FS was supported by NSF 1919566 and NASA NNX17AI03G. HS and SN were supported by grants from NASA Cryospheric Science, Modeling, Analysis and Prediction Programs, and Sea Level Change Team Programs.

References

Asay-Davis, X. S., Jourdain, N. C., and Nakayama, Y.: Developments in Simulating and Parameterizing Interactions Between the Southern Ocean and the Antarctic Ice Sheet, Current Climate Change Reports, 3, 316–329, 2017.

Bamber, J. L., Westaway, R. M., Marzeion, B., and Wouters, B.: The land ice contribution to sea level during the satellite era, Environmental Research Letters, 13, 063 008, 2018.

Barthel, A., Agosta, C., Little, C. M., Hatterman, T., Jourdain, N. C., Goelzer, H., Nowicki, S., Seroussi, H., Straneo, F., and Bracegirdle, T. J.: CMIP5 model selection for ISMIP6 ice sheet model forcing: Greenland and Antarctica, The Cryosphere Discussions, 00, 1–34, https://doi.org/10.5194/tc-2019-191, https://www.the-cryosphere-discuss.net/tc-2019-191/, 2019.

Bindschadler, R. A., Nowicki, S., Abe-Ouchi, A., Aschwanden, A., Choi, H., Fastook, J., Granzow, G., Greve, R., Gutowski, G., Herzfeld, U., et al.: Ice-sheet model sensitivities to environmental forcing and their use in projecting future sea level (the SeaRISE project), J. Glaciology, 59, 195, 2013.

Bracegirdle, T. J., Shuckburgh, E., Sallee, J.-B., Wang, Z., Meijers, A. J. S., Bruneau, N., Phillips, T., and Wilcox, L. J.: Assessment of surface winds over the Atlantic, Indian, and Pacific Ocean sectors of the Southern Ocean in CMIP5 models: Historical bias, forcing response, and state dependence, J. Geophys. Res. Atmospheres, 118, 547–562, 2013.

Bronselaer, B., Winton, M., Griffies, S. M., Hurlin, W. J., Rodgers, K. B., Sergienko, O. V., Stouffer, R. J., and Russell, J. L.: Change in future climate due to Antarctic meltwater, Nature, 564, 53, 2018.

Cornford, S. L., Martin, D. F., Payne, A. J., Ng, E. G., Le Brocq, A. M., Gladstone, R. M., Edwards, T. L., Shannon, S. R., Agosta, C., van den Broeke, M. R., et al.: Century-scale simulations of the response of the West Antarctic Ice Sheet to a warming climate, The Cryosphere, 9, 2015.

Dansereau, V., Heimbach, P., and Losch, M.: Simulation of subice shelf melt rates in a general circulation model: Velocity-dependent transfer and the role of friction, J. Geophys. Res., 119, 1765–1790, 2014.

De Rydt, J. and Gudmundsson, G. H.: Coupled ice shelf-ocean modeling and complex grounding line retreat from a seabed ridge, J. Geophys. Res., 121, 865–880, 2016.

De Rydt, J., Holland, P. R., Dutrieux, P., and Jenkins, A.: Geometric and oceanographic controls on melting beneath Pine Island Glacier, J. Geophys. Res., 119, 2420–2438, 2014.

DeConto, R. M. and Pollard, D.: Contribution of Antarctica to past and future sea-level rise, Nature, 531, 591, 2016.

Depoorter, M. A., Bamber, J. L., Griggs, J. A., Lenaerts, J. T. M., Ligtenberg, S. R. M., van den Broeke, M. R., and Moholdt, G.: Calving fluxes and basal melt rates of Antarctic ice shelves, Nature, 502, 89–92, 2013.

Donat-Magnin, M., Jourdain, N. C., Spence, P., Le Sommer, J., Gallée, H., and Durand, G.: Ice-Shelf Melt Response to Changing Winds and Glacier Dynamics in the Amundsen Sea Sector, Antarctica, J. Geophys. Res., 122, 10 206–10 224, 2017.

Dutrieux, P., De Rydt, J., Jenkins, A., Holland, P. R., Ha, H. K., Lee, S. H., Steig, E. J., Ding, Q., Abrahamsen, E. P., and Schröder, M.: Strong sensitivity of Pine Island ice-shelf melting to climatic variability, Science, 343, 174–178, 2014.

Eyring, V., Bony, S., Meehl, G. A., Senior, C. A., Stevens, B., Stouffer, R. J., and Taylor, K. E.: Overview of the Coupled Model Intercomparison Project Phase 6 (CMIP6) experimental design and organization, Geoscientific Model Development, 9, 1937–1958, 2016.

Favier, L., Durand, G., Cornford, S. L., Gudmundsson, G. H., Gagliardini, O., Gillet-Chaulet, F., Zwinger, T., Payne, A. J., and Le Brocq, A. M.: Retreat of Pine Island Glacier controlled by marine ice-sheet instability, Nature Climate Change, 4, 117–121, 2014.

Favier, L., Jourdain, N. C., Jenkins, A., Merino, N., Durand, G., Gagliardini, O., Gillet-Chaulet, F., and Mathiot, P.: Assessment of Sub-Shelf Melting Parameterisations Using the Ocean-Ice Sheet Coupled Model NEMO (v3. 6)-Elmer/Ice (v8. 3), Geoscientific Model Development, 2019.

Fretwell, P., Pritchard, H. D., Vaughan, D. G., Bamber, J. L., Barrand, N. E., Bell, R., Bianchi, C., Bingham, R. G., Blankenship, D. D., Casassa, G., et al.: Bedmap2: improved ice bed, surface and thickness datasets for Antarctica, The Cryosphere, 7, 2013.

Gillet-Chaulet, F., Gagliardini, O., Seddik, H., Nodet, M., Durand, G., Ritz, C., Zwinger, T., Greve, R., and Vaughan, D. G.: Greenland ice sheet contribution to sea-level rise from a new-generation ice-sheet model, The Cryosphere, 6, 1561–1576, 2012.

Goelzer, H., Huybrechts, P., Fürst, J. J., Nick, F. M., Andersen, M. L., Edwards, T. L., Fettweis, X., Payne, A. J., and Shannon, S.: Sensitivity of Greenland ice sheet projections to model formulations, J. Glaciology, 59, 733–749, 2013.

Golledge, N. R., Keller, E. D., Gomez, N., Naughten, K. A., Bernales, J., Trusel, L. D., and Edwards, T. L.: Global environmental consequences of twenty-first-century ice-sheet melt, Nature, 566, 65, 2019.

Good, S. A., Martin, M. J., and Rayner, N. A.: EN4: Quality controlled ocean temperature and salinity profiles and monthly objective analyses with uncertainty estimates, J. Geophys. Res. Oceans, 118, 6704–6716, 2013.

Gudmundsson, G. H.: Ice-shelf buttressing and the stability of marine ice sheets, The Cryosphere, 7, 647–655, https://doi.org/https://doi.org/10.5194/tc-7-647-2013, 2013.

Hattermann, T.: Antarctic Thermocline Dynamics along a Narrow Shelf with Easterly Winds, J. Phys. Oceanogr., 48, 2419–2443, 2018.

Hattermann, T. and Levermann, A.: Response of Southern Ocean circulation to global warming may enhance basal ice shelf melting around Antarctica, Climate Dynam., 35, 741–756, 2010.

Hellmer, H. H., Kauker, F., Timmermann, R., Determann, J., and Rae, J.: Twenty-first-century warming of a large Antarctic ice-shelf cavity by a redirected coastal current, Nature, 485, 225, 2012.

Hellmer, H. H., Kauker, F., Timmermann, R., and Hattermann, T.: The fate of the southern Weddell Sea continental shelf in a warming climate, J. Climate, 30, 4337–4350, 2017.

Holland, D. M. and Jenkins, A.: Modeling thermodynamic ice-ocean interactions at the base of an ice shelf, J. Phys. Oceanogr., 29, 1787–1800, 1999.

Holland, P. R., Jenkins, A., and Holland, D. M.: The response of ice shelf basal melting to variations in ocean temperature, J. Climate, 21, 2558–2572, 2008.

Iversen, T., Bentsen, M., Bethke, I., Debernard, J. B., Kirkevåg, A., Seland, Ø., Drange, H., Kristjansson, J. E., Medhaug, I., Sand, M., and Seierstad, I. A.: The Norwegian Earth System Model, NorESM1-M - Part 2: Climate response and scenario projections, Geoscientific Model Development, 6, 389–415, https://doi.org/10.5194/gmd-6-389-2013, https://www.geosci-model-dev.net/6/389/2013/, 2013.

Jacobs, S. S., Jenkins, A., Giulivi, C. F., and Dutrieux, P.: Stronger ocean circulation and increased melting under Pine Island Glacier ice shelf, Nature Geoscience, 4, 519–523, 2011.

Jenkins, A.: A one-dimensional model of ice shelf-ocean interaction, J. Geophys. Res., 96, 20 671–20 677, 1991.

Jenkins, A., Nicholls, K. W., and Corr, H. F. J.: Observation and parameterization of ablation at the base of Ronne Ice Shelf, Antarctica, J. Phys. Oceanogr., 40, 2298–2312, 2010.

Jenkins, A., Shoosmith, D., Dutrieux, P., Jacobs, S., Kim, T. W., Lee, S. H., Ha, H. K., and Stammerjohn, S.: West Antarctic Ice Sheet retreat in the Amundsen Sea driven by decadal oceanic variability, Nature Geosc., 11, 733–738, 2018.

Joughin, I., Smith, B. E., and Medley, B.: Marine ice sheet collapse potentially under way for the Thwaites Glacier Basin, West Antarctica, Science, 344, 735–738, 2014.

Jourdain, N. C., Mathiot, P., Merino, N., Durand, G., Le Sommer, J., Spence, P., Dutrieux, P., and Madec, G.: Ocean circulation and sea-ice thinning induced by melting ice shelves in the Amundsen Sea, J. Geophys. Res. Oceans, 122, 2550–2573, 2017.

Krinner, G. and Flanner, M. G.: Striking stationarity of large-scale climate model bias patterns under strong climate change, Proceedings of the National Academy of Sciences, 115, 9462–9466, 2018.

Lazeroms, W. M. J., Jenkins, A., Gudmundsson, G. H., and Van De Wal, R. S. W.: Modelling present-day basal melt rates for Antarctic ice shelves using a parametrization of buoyant meltwater plumes, The Cryosphere, 12, 49–70, 2018.

Lazeroms, W. M. J., Jenkins, A., Rienstra, S. W., and van de Wal, R. S. W.: An analytical derivation of ice-shelf basal melt based on the dynamics of meltwater plumes, J. Phys. Oceanogr., 49, 917–939, 2019.

Little, C. M. and Urban, N. M.: CMIP5 temperature biases and 21st century warming around the Antarctic coast, Annals of Glaciology, 57, 69–78, 2016.

Little, C. M., Gnanadesikan, A., and Oppenheimer, M.: How ice shelf morphology controls basal melting, J. Geophys. Res., 114, 2009.

Locarnini, R. A., Mishonov, A. V., Baranova, O. K., Boyer, T. P., Zweng, M. M., Garcia, H. E., Reagan, J. R., Seidov, D., Weathers, K. W., Paver, C. R., and Smolyar, I. V.: World Ocean Atlas 2018, Volume 1: Temperature, Tech. Rep. Atlas NESDIS 81, NOAA, https://data.nodc.noaa.gov/woa/WOA18/DOC/woa18_vol1.pdf, 2019.

MacAyeal, D. R., Okal, E. A., Aster, R. C., Bassis, J. N., Brunt, K. M., Cathles, L. M., Drucker, R., Fricker, H. A., Kim, Y.-J., Martin, S., Okal, M. H., Sergienko, O. V., Sponsler, M. P., and Thom, J. E.: Transoceanic wave propagation links iceberg calving margins of Antarctica with storms in tropics and Northern Hemisphere, Geophys. Res. Lett., 33, 1–4, https://doi.org/10.1029/2006GL027235, 2006.

Massom, R. A., Scambos, T. A., Bennetts, L. G., Reid, P., Squire, V. A., and Stammerjohn, S. E.: Antarctic ice shelf disintegration triggered by sea ice loss and ocean swell, Nature, 558, 383, 2018.

McDougall, T. J. and Barker, P. M.: Getting started with TEOS-10 and the Gibbs Seawater (GSW) oceanographic toolbox, SCOR/IAPSO WG, 127, 1–28, 2011.

Meredith, M. P.: The global importance of the Southern Ocean and the key role of its freshwater cycle, Ocean Challenge, 23, 27–33, https://www.challenger-society.org.uk/oceanchallenge/2019_23_2.pdf, 2019.

Millan, R., Rignot, E., Bernier, V., Morlighem, M., and Dutrieux, P.: Bathymetry of the Amundsen Sea Embayment sector of West Antarctica from Operation IceBridge gravity and other data, Geophys. Res. Lett., 44, 1360–1368, 2017.

Mouginot, J., Scheuchl, B., and Rignot, E.: MEaSUREs Antarctic Boundaries for IPY 2007-2009 from Satellite Radar, Version 2, Tech. rep., Boulder, Colorado USA. NASA National Snow and Ice Data Center Distributed Active Archive Center, https://doi.org/10.5067/AXE4121732AD, https://nsidc.org/data/nsidc-0709/versions/2, 2017.

Nakayama, Y., Timmermann, R., Schröder, M., and Hellmer, H. H.: On the difficulty of modeling Circumpolar Deep Water intrusions onto the Amundsen Sea continental shelf, Ocean Modelling, 84, 26–34, 2014.

Naughten, K. A., Meissner, K. J., Galton-Fenzi, B. K., England, M. H., Timmermann, R., and Hellmer, H. H.: Future projections of Antarctic ice shelf melting based on CMIP5 scenarios, J. Climate, 31, 5243–5261, 2018a.

Naughten, K. A., Meissner, K. J., Galton-Fenzi, B. K., England, M. H., Timmermann, R., Hellmer, H. H., Hattermann, T., and Debernard, J. B.: Intercomparison of Antarctic ice-shelf, ocean, and sea-ice interactions simulated by MetROMS-iceshelf and FESOM 1.4, Geoscientific Model Development, 11, 1257–1292, 2018b.

Nowicki, S., Bindschadler, R. A., Abe-Ouchi, A., Aschwanden, A., Bueler, E., Choi, H., Fastook, J., Granzow, G., Greve, R., Gutowski, G., et al.: Insights into spatial sensitivities of ice mass response to environmental change from the SeaRISE ice sheet modeling project I: Antarctica, J. Geophys. Res. Earth Surface, 118, 1002–1024, 2013.

Nowicki, S. M. J., Payne, A., Larour, E., Seroussi, H., Goelzer, H., Lipscomb, W., Gregory, J., Abe-Ouchi, A., and Shepherd, A.: Ice Sheet Model Intercomparison Project (ISMIP6) contribution to CMIP6, Geoscientific Model Development, 9, 4521, 2016.

Padman, L., Siegfried, M. R., and Fricker, H. A.: Ocean Tide Influences on the Antarctic and Greenland Ice Sheets, Reviews of Geophysics, 56, 1–43, 2018.

Pattyn, F., Perichon, L., Durand, G., Favier, L., Gagliardini, O., Hindmarsh, R. C. A., Zwinger, T., Albrecht, T., Cornford, S. L., Docquier, D., et al.: Grounding-line migration in plan-view marine ice-sheet models: results of the ice2sea MISMIP3d intercomparison, J. Glaciology, 59, 410–422, 2013.

Pelle, T., Morlighem, M., and Bondzio, J. H.: Brief communication: PICOP, a new ocean melt parameterization under ice shelves combining PICO and a plume model, The Cryosphere, 13, 1043–1049, 2019.

Pollard, D., DeConto, R. M., and Alley, R. B.: Potential Antarctic Ice Sheet retreat driven by hydrofracturing and ice cliff failure, Earth Planet. Sc. Lett., 412, 112–121, 2015.

Pritchard, H. D., Ligtenberg, S. R. M., Fricker, H. A., Vaughan, D. G., Van den Broeke, M. R., and Padman, L.: Antarctic ice-sheet loss driven by basal melting of ice shelves, Nature, 484, 502–505, 2012.

Reese, R., Albrecht, T., Mengel, M., Asay-Davis, X., and Winkelmann, R.: Antarctic sub-shelf melt rates via PICO, The Cryosphere, 12, 1969–1985, 2018a.

Reese, R., Gudmundsson, G. H., Levermann, A., and Winkelmann, R.: The far reach of ice-shelf thinning in Antarctica, Nature Climate Change, 8, 53, 2018b.

Rignot, E., Jacobs, S., Mouginot, J., and Scheuchl, B.: Ice-shelf melting around Antarctica, Science, 341, 266–270, 2013.

Rignot, E., Mouginot, J., Scheuchl, B., van den Broeke, M., van Wessem, M. J., and Morlighem, M.: Four decades of Antarctic Ice Sheet mass balance from 1979–2017, Proceedings of the National Academy of Sciences, 116, 1095–1103, 2019.

Rintoul, S. R., Silvano, A., Pena-Molino, B., van Wijk, E., Rosenberg, M., Greenbaum, J. S., and Blankenship, D. D.: Ocean heat drives rapid basal melt of the Totten Ice Shelf, Science Advances, 2, e1601 610, 2016.

Ritz, C., Edwards, T. L., Durand, G., Payne, A. J., Peyaud, V., and Hindmarsh, R. C. A.: Potential sea-level rise from Antarctic ice-sheet instability constrained by observations, Nature, 528, 115–118, 2015.

Roquet, F., Wunsch, C., Forget, G., Heimbach, P., Guinet, C., Reverdin, G., Charrassin, J.-B., Bailleul, F., Costa, D. P., Huckstadt, L. A., et al.: Estimates of the Southern Ocean general circulation improved by animal-borne instruments, Geophys. Res. Lett., 40, 6176–6180, 2013.

Roquet, F., Williams, G., Hindell, M. A., Harcourt, R., McMahon, C., Guinet, C., Charrassin, J.-B., Reverdin, G., Boehme, L., Lovell, P., et al.: A Southern Indian Ocean database of hydrographic profiles obtained with instrumented elephant seals, Scientific data, 1, 140 028, 2014.

Sallée, J. B., Shuckburgh, E., Bruneau, N., Meijers, A. J., Bracegirdle, T. J., Wang, Z., and Roy, T.: Assessment of Southern Ocean water mass circulation and characteristics in CMIP5 models: Historical bias and forcing response, J. Geophys. Res. Oceans, 118, 1830–1844, 2013.

Scambos, T., Fricker, H. A., Liu, C.-C., Bohlander, J., Fastook, J., Sargent, A., Massom, R., and Wu, A.-M.: Ice shelf disintegration by plate bending and hydro-fracture: Satellite observations and model results of the 2008 Wilkins ice shelf break-ups, Earth and Planetary Science Letters, 280, 51–60, 2009.

Schaffer, J., Timmermann, R., Arndt, J. E., Kristensen, S. S., Mayer, C., Morlighem, M., and Steinhage, D.: A global high-resolution data set of ice sheet topography, cavity geometry and ocean bathymetry, Earth System Science Data, 2016.

Schloesser, F., Friedrich, T., Timmermann, A., DeConto, R. M., and Pollard, D.: Antarctic iceberg impacts on future Southern Hemisphere climate, Nature Climate Change, pp. 1–6, 2019.

Seroussi, H., Morlighem, M., Rignot, E., Mouginot, J., Larour, E., Schodlok, M., and Khazendar, A.: Sensitivity of the dynamics of Pine Island Glacier, West Antarctica, to climate forcing for the next 50 years, The Cryosphere, 8, 1699–1710, 2014.

Seroussi, H., Nakayama, Y., Larour, E., Menemenlis, D., Morlighem, M., Rignot, E., and Khazendar, A.: Continued retreat of Thwaites Glacier, West Antarctica, controlled by bed topography and ocean circulation, Geophysical Research Letters, 44, 6191–6199, 2017.

Seroussi, H., Nowicki, S., Simon, E., Abe-Ouchi, A., Albrecht, T., Brondex, J., Cornford, S., Dumas, C., Gillet-Chaulet, F., Goelzer, H., et al.: initMIP-Antarctica: an ice sheet model initialization experiment of ISMIP6, The Cryosphere, 13, 1441–1471, 2019.

Shepherd, A., Ivins, E., Rignot, E., Smith, B., Van Den Broeke, M., Velicogna, I., Whitehouse, P., Briggs, K., Joughin, I., Krinner, G., et al.: Mass balance of the Antarctic Ice Sheet from 1992 to 2017, Nature, 558, 219–222, 2018.

Snow, K., Goldberg, D. N., Holland, P. R., Jordan, J. R., Arthern, R. J., and Jenkins, A.: The response of ice sheets to climate variability, Geophysical Research Letters, 44, 11–878, 2017.

St-Laurent, P., Klinck, J. M., and Dinniman, M. S.: On the role of coastal troughs in the circulation of warm Circumpolar Deep Water on Antarctic shelves, J. Phys. Oceanogr., 43, 51–64, 2013.

Stewart, A. L., Klocker, A., and Menemenlis, D.: Circum-Antarctic Shoreward Heat Transport Derived From an Eddy-and Tide-Resolving Simulation, Geophys. Res. Lett., 2018.

Swingedouw, D., Fichefet, T., Huybrechts, P., Goosse, H., Driesschaert, E., and Loutre, M.-F.: Antarctic ice-sheet melting provides negative feedbacks on future climate warming, Geophys Res Lett, 35, 2008.

Timmermann, R. and Goeller, S.: Response to Filchner–Ronne Ice Shelf cavity warming in a coupled ocean–ice sheet model–Part 1: The ocean perspective, Ocean Science, 13, 765–776, 2017.

Timmermann, R. and Hellmer, H. H.: Southern Ocean warming and increased ice shelf basal melting in the twenty-first and twenty-second centuries based on coupled ice-ocean finite-element modelling, Ocean Dynamics, 63, 1011–1026, 2013.

Treasure, A. M., Roquet, F., Ansorge, I. J., Bester, M. N., Boehme, L., Bornemann, H., Charrassin, J.-B., Chevallier, D., Costa, D. P., Fedak, M. A., et al.: Marine mammals exploring the oceans pole to pole: a review of the MEOP consortium, Oceanography, 30, 132–138, 2017.

Turner, J., Bracegirdle, T. J., Phillips, T., Marshall, G. J., and Hosking, J. S.: An initial assessment of Antarctic sea ice extent in the CMIP5 models, J. Climate, 26, 1473–1484, 2013.

van den Broeke, M.: Strong surface melting preceded collapse of Antarctic Peninsula ice shelf, Geophys. Res. Lett., 32, 2005.

Vaughan, D. G., Marshall, G. J., Connolley, W. M., Parkinson, C., Mulvaney, R., Hodgson, D. A., King, J. C., Pudsey, C. J., and Turner, J.: Recent rapid regional climate warming on the Antarctic Peninsula, Climatic change, 60, 243–274, 2003.

Zweng, M. M., Reagan, J. R., Seidov, D., Boyer, T. P., Locarnini, R., Garcia, H. E., Mishonov, A. V., Baranova, O. K., Weathers, K. W., Paver, C. R., and Smolyar, I. V.: World Ocean Atlas 2018, Volume 2: Salinity, Tech. Rep. Atlas NESDIS 82, NOAA, https://data.nodc.noaa.gov/woa/WOA18/DOC/woa18_vol2.pdf, 2019.